THESIS APPROVAL

GRADUATE SCHOOL, KASETSART UNIVERSITY

Master of Science (Packaging Technology)

DEGREE

Packaging Technology — **FIELD**

Packaging and Materials Technology — **DEPARTMENT**

TITLE: Effect of Chitosan on Properties of Thermoplastic Starch Blown Film

NAME: Mr. Khanh Minh Dang

THIS THESIS HAS BEEN ACCEPTED BY

(Assistant Professor Rangrong Yoksan, Ph.D.) **THESIS ADVISOR**

(Assistant Professor Amporn Sane, Ph.D.) **THESIS CO-ADVISOR**

(Assistant Professor Namfone Lumdubwong, Ph.D.) **THESIS CO-ADVISOR**

(Assistant Professor Tunyarut Jinkarn, Ph.D.) **DEPARTMENT HEAD**

APPROVED BY THE GRADUATE SCHOOL ON _____

(Associate Professor Gunjana Theeragool, D.Agr.) **DEAN**

THESIS

EFFECT OF CHITOSAN ON PROPERTIES OF THERMOPLASTIC STARCH BLOWN FILM

KHANH MINH DANG

A Thesis Submitted in Partial Fulfillment of
the Requirements for the Degree of
Master of Science (Packaging Technology)
Graduate School, Kasetsart University
2014

Khanh Minh Dang 2014: Effect of Chitosan on Properties of Thermoplastic Starch Blown Film. Master of Science (Packaging Technology), Major Field: Packaging Technology, Department of Packaging and Materials Technology. Thesis Advisor: Assistant Professor Rangrong Yoksan, Ph.D. 68 pages.

The objective of the present thesis is to improve blown film extrusion processability and properties of thermoplastic starch (TPS) film by incorporating chitosan (CTS) with 0.5-2 part(s) per hundred parts of starch (phs). TPS/CTS compounds were prepared using a twin-screw extruder followed by blowing into a film via blown film extrusion. The effect of chitosan on blown film extrusion processability, optical properties, morphology, thermal properties, tensile properties as well as water vapor and oxygen permeability of the films was investigated. The possible interactions between starch and chitosan molecules were evaluated by FTIR and XRD techniques. Starch and chitosan molecules could interact via hydrogen bonds as confirmed from the blue shift of OH bands and the reduction of V-type starch crystal formation. Glass-transition temperature evaluated by DSC and DMTA tended to increase as a function of chitosan content. Although the incorporation of chitosan caused decreased extensibility as well as increased yellowness and opacity, the films exhibited increased tensile strength, rigidity, thermal stability and UV absorption, improved water vapor and oxygen barrier properties, as well as reduced water absorption and surface stickiness. The obtained TPS/CTS films offer great potential applications in food industry as edible films.

_____ / ___ / ___

Student's signature Thesis Advisor's signature

ACKNOWLEDGEMENTS

I would like to express the deepest appreciation to my advisor, Assistant Professor Rangrong Yoksan, who always motivates and encourages me to complete not only doing experiments, but also writing this thesis book. Without her guidance and persistent help this thesis would not have been possible. I would sincerely like to thank my committees, Assistant Professor Amporn Sane and Assistant Professor Namfone Lumdubwong and the Graduate School representative, Assistant Professor Lerpong Jarupan as well as the external committee, Professor Suwabun Chirachanchai for their useful and valuable comments and suggestions.

In addition, I also would like to acknowledge Assistant Professor Tunyarut Jinkarn and Associate Professor Vanee Chohenchob for giving me a good chance to study at the Department of Packaging and Materials Technology. I heartfelt thank the technicians, Ms. Tanthip Chreanpakdee and Mr. Kittichai Tansin as well as all of my friends for their supports. I am also appreciated my family for their continuing encouragement.

Last but not least, I would like to thank the Faculty of Agro-Industry, Kasetsart University for supporting me the Scholarship for International Student.

Khanh Minh Dang

April 2014

TABLE OF CONTENTS

Page

LIST OF TABLES

LIST OF FIGURES

LIST OF FIGURES (Continued)

LIST OF ABBREVIATIONS

CTS	=	Chitosan
DMTA	=	Dynamic mechanical thermal analysis
DSC	=	Differential scanning calorimetry
FTIR	=	Fourier transform infrared spectroscopy
L/D	=	Length/Diameter
MFI	=	Melt flow index
OP	=	Oxygen permeability
OTR	=	Oxygen transmission rate
TGA	=	Thermogravimetric analysis
TPS	=	Thermoplastic starch
WVP	=	Water vapor permeability
WVTR	=	Water vapor transmission rate
XRD	=	X-ray diffraction analysis

EFFECT OF CHITOSAN ON PROPERTIES OF THERMOPLASTIC STARCH BLOWN FILM

INTRODUCTION

Nowadays, the growing accumulation of non-biodegradable plastic waste together with the difficulty of recycling the plastic packaging has stimulated the development of biodegradable packaging from renewable resources. Due to its complete biodegradability, low cost and worldwide availability. However, starch-based films present poor water vapor barrier and mechanical properties. Although the addition of plasticizers such as glycerol or sorbitol has been reported to reduce the stiffness or improve the flexibility of the films, their permeability to water vapor still be the problem remained. The incorporation of chitosan is expected to be an alternative to improve water vapor barrier and mechanical properties of the starch-based film due to the formation of intermolecular hydrogen bonding between chitosan and starch. In addition, chitosan is not only nontoxic and biodegradable material, but also possesses antimicrobial property as well as has the potential to be used as a major raw material for the production of biodegradable film.

Solution casting is the most widely used technique to prepare starch/chitosan-based films in the research areas. However, the need of a large amount of solvent, time consuming and low productivity efficiency of solution casting method are drawbacks for its applying in industrial level. Blown film extrusion is an alternative option to approach the industrial goal since it employs the existing machines for conventional plastics and possesses high productivity efficiency.

However, blending starch with chitosan flakes using an extruder cannot provide homogeneous material because chitosan cannot melt leading to the incomplete mix with thermoplastic starch. Therefore, the objective of the present thesis is to enhance blown film extrusion processability and improve barrier and tensile properties of thermoplastic starch film by incorporating chitosan in the solution form.

OBJECTIVES

1. To enhance blown film extrusion processability and improve barrier and tensile properties of thermoplastic starch film by incorporating chitosan in the solution form

2. To study the effect of chitosan on characteristics and properties of thermoplastic starch blown film

Thesis scopes

1. Prepare thermoplastic starch/chitosan compounds by twin screw extruder

2. Prepare thermoplastic starch/chitosan films by film blowing machine

3. Characterize and test the properties of thermoplastic starch/chitosan compounds and films

LITERATURE REVIEW

1. Starch

Starches are the main storage polysaccharides in foods of plant origin. The total utilization of worldwide dried starch was actually estimated at 71 million tons and almost 81.3 million tons by 2015. Current annual production for primary starch sources is estimated to be 46.1 million tons for corn (73%), 9.1 million tons for cassava (14%), 5.15 million tons for wheat (8%), and 2.45 million tons for potato (4%) (Figure 1) (Röper and Elvers, 2008).

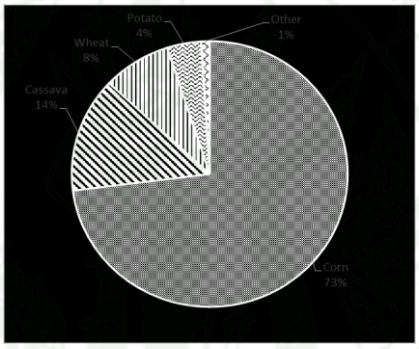

Figure 1 Starch production according to botanic.

Sources: Röper and Elvers (2008)

Starch can be found in various parts of plants such as seeds, roots and tubers, and also found in stems, leaves, fruits and even pollen (Carvalho, 2008). The diameters of granules basically range from 1 μm to more than 100 μm (Bertolini, 2010) and shapes can be regular (e.g. spherical, ovoid, or angular) or irregular. In general, starch granules are partially crystalline particles composed mainly of two homopolymers of glucopyranose with different structures, namely amylose and amylopectin (Figure 2) (French, 1973). Amylose is a predominantly α-D-(1-4) glucopyranosyl linear macromolecule (Figure 2a) and possesses a degree of polymerization (DP) as high as 600 monomeric units. Most commercial starches (e.g. potato, corn) contain about 25% amylose, the remainder being amylopectin (French,

1973). Amylopectin, which is a major component of the starch granule (30–99%), is a highly branched (Figure 2b) and high molecular weight macromolecule composed mostly of α-D-(1-4)-glucopyranose units and α-(1-6)-linkages (Carvalho, 2008). With a molecular weight ranging from 50–500 $\times 10^6$ units, amylopectin is one of the largest natural polymers known.

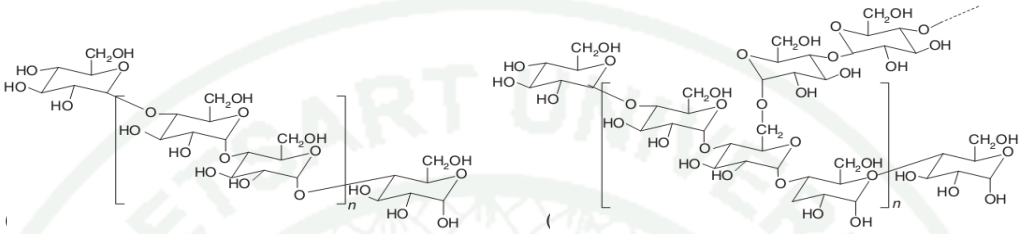

(a) (b)

Figure 2 Chemical structures of (a) amylose and (b) amylopectin.

Table 1 Size, shape and amylose content of some starch granules.

Source	Diameter (μm)	Amylose content (wt%)	Shape
Maize	5–25	28	Polyhedric
Waxy maize	5–25	0	Polyhedric
High-amylose	5–35	55–85	Varied smooth spherical to elongated
Cassava	5–35	16	Semi-spherical
Potato	15–100	20	Ellipsoidal
Wheat	20–22	30	Lenticular, polyhedric
Normal rice	3–8	20–30	Polyhedric
Banana	26–35	9–13	Elongated oval with ridges

Source: Carvalho (2008)

Starch can be classified to A, B and C crystallites or polymorph forms, each type presenting its characteristic diffraction patterns. The most commonly observed

structures in native starch are A and B, the former being associated mainly with cereal starches, while the latter dominates generally in tuber starches but also occurs in maize starches with amylose content of more than 30-40% (Blanshard, 1987). The C–type pattern is an intermediate form between A and B and is usually associated with pea and various bean starches together with other root starches (Colonna *et al.*, 1987). A–type crystallites are denser and less hydrated than B–type counterparts, whereas the C–type crystallites arise from the joint presence of the other two homologues (Colonna *et al.*, 1987).

The semi-crystalline nature of starch is important in the alternation of long range molecular order and amorphous regions (Carvalho, 2008). Its properties are related to the short-chain fraction of amylopectin arranged as double helices and packed in small crystallites. Linear amylose molecules are apparently present in an amorphous state in the granule (Bertolini, 2010) (Figure 3).

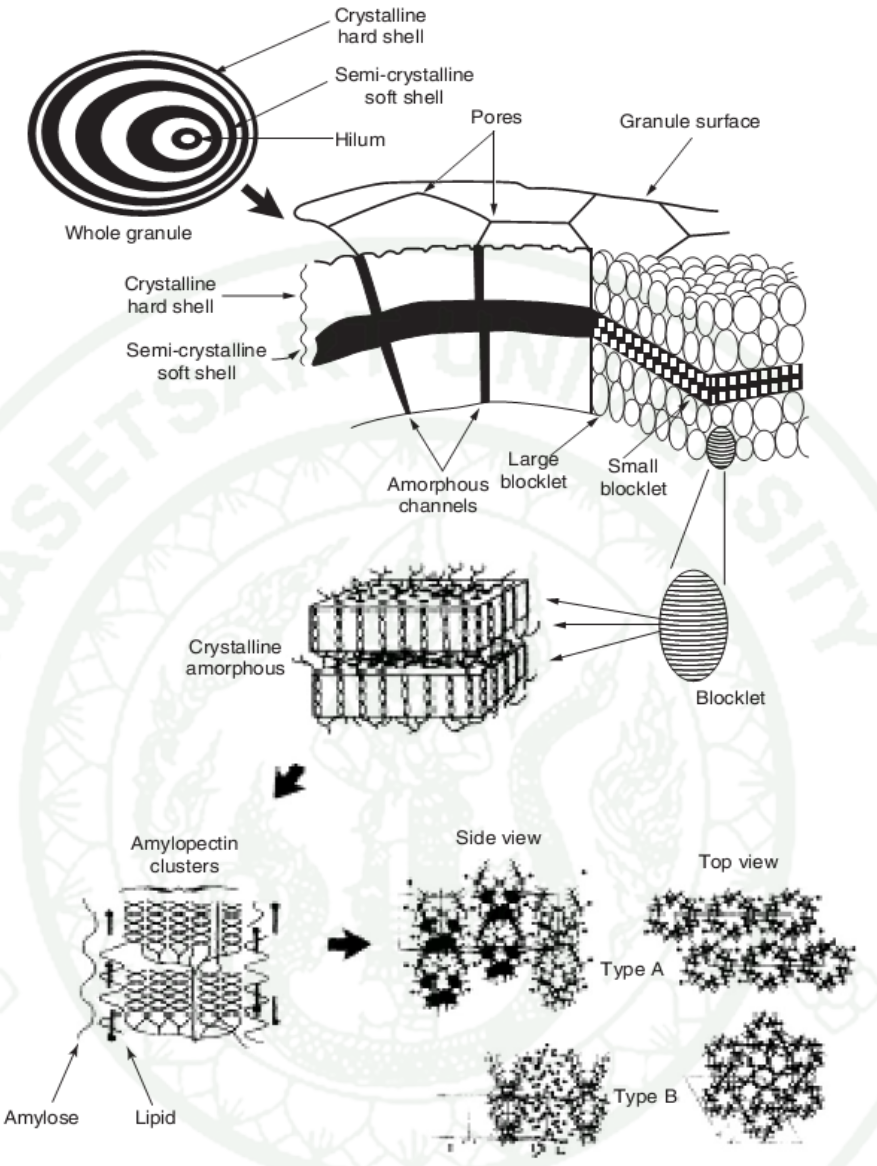

Figure 3 Starch granule structure.

Source: Gallant *et al.* (1997)

1.1 Thermoplastic starch (TPS)

In general, native starches are non-plastic materials due to the intra- and intermolecular hydrogen bonds formed between the hydroxyl groups of starch molecules, which promote their crystallinity. The penetration of plasticizers into the starch granules can disrupt the initial crystallographic structure of starch. In addition,

under applying heat and shear forces, the material undergoes a melting process and forms a continuous amorphous mass that no longer diffraction (Avérous, 2004).

Thermoplastic starch (TPS) can be prepared by using different starch types such as wheat starch (Huneault and Li, 2012), potato starch (Mościcki *et al.*, 2012), rice starch (Prachayawarakorn *et al.*, 2010) and cassava starch (Pelissari *et al.*, 2012). There are many plasticizers such as glycerol (Huneault and Li, 2012), sorbitol, propylene and ethylene glycol (Roz *et al.*, 2006) has been used to prepare TPS.

After thermo-mechanical process, the crystalline order observed in the native starch granules is completely destroyed leading to the mobility of the starch chains, followed by their recrystallization to form B-, V- and E-type crystalline structures. B-type appears after TPS is stored above its glass transition temperature or at high moisture contents (Carvalho, 2008; Soest and Essers, 1997). V- and E-types are observed just after extrusion and are generated during processing. V-type structures formed by amylose and can be observed in two forms: V_a-type (anhydrous) for materials containing low moisture contents and V_h-type (hydrated) for materials containing higher moisture contents (Soest and Essers, 1997). E-type occurs only in materials with low moisture content and is not stable; it changes into V_h–type at ambient temperature with more than 30 percent relative humidity during storage. The total amount of amylose crystallinity remains the same (Carvalho, 2008).

TPS stands out amongst other polymers because it possesses low price, non-toxicity, biodegradability and composability as well as it derives from renewable resources. However, the use of TPS has been very limited because of its poor water resistance due to its hydrophilicity and poor mechanical performances. Blending/mixing TPS with other materials probably overcomes these limitations and reduces the cost of the ensuing blends as well. Many kinds of polymers have been used to blend/mix with TPS such as PE (Shujun *et al.*, 2006), PLA (Teixeira *et al.*, 2012), PBAT (Brandelero *et al.*, 2012) and chitosan (Pelissari *et al.*, 2012).

TPS can be converted into various shaped and sized products by using thermal processes such as injection molding (Mościcki *et al.*, 2012), compression

molding (Kaewtatip and Thongmee, 2013), sheet extrusion (Dean *et al.*, 2007), thermoforming process (Avérousa *et al.*, 2001) and blown film extrusion (Mościcki *et al.*, 2012).

Among those techniques, blown film extrusion is an enormous potential technique used for converting plastics, including TPS into flexible packaging, e.g. films, bags. Recently, the blown film extrusion has become commonly popular for producing films because of its high productivity. Therefore, many studies about the film blowing of thermoplastic starch have been reported (Mościcki *et al.*, 2012; Thunwall *et al.*, 2008; Zullo and Iannace, 2009).

Thunwall *et al.* (2008) investigated the feasibility of film blowing of the materials composed of starch, glycerol and water. The main objective of this study was to establish the film by using those materials and to estimate the processing window, i.e. the conditions which limit the processability such as amount of glycerol and moisture content. Two potato starch grades, which were native (natural) grade and oxidized and hydroxypropylated grade were employed. Starch and glycerol were mixed and blown into a film by a single screw extruder (L=11D). The screw speed was 24 rpm and temperature profile was in the range of 90–160 °C. Starch and glycerol were mixed using a ratio of starch:glycerol of 100:15, 100:22, 100:30 and 100:45 (w/w). The results showed that it was possible, without any significant problems, to blow the oxidized and hydroxypropylated starch based materials with high glycerol content, i.e. 45 parts per 100 parts of dry starch. However, due to the sticky surface of the extruded material, a double-walled film, which is impossible to separate, was obtained after passage through the calendering nip. Reducing the moisture content by drying the pellets prior to the film blowing could reduce the problem but not to a sufficient extent. Simultaneously, the torque required from the extruder and the die pressure increased significantly due to the lower moisture content (giving a higher viscosity). A material based on 100 parts of dried oxidized and hydroxypropylated starch, 22 parts of glycerol and 10% of moisture was found to be a reasonable compromise because a double-walled glued film was avoided while a sufficient expansion potential was still maintained. Mechanical properties in the

parallel and perpendicular to flow direction were clearly different. Tensile strength and modulus were higher in the flow direction whereas the strain at break was lower, indicating that the film were anisotropic. The films shrank about 26% in the flow direction and 17% in the perpendicular direction during storage for a month at room temperature at 53% RH.

Zullo and Iannace (2009) studied the effect of different starch sources (maize, potato and wheat) and plasticizer types (glycerol, urea and formamide) and their contents on the physico-chemical and mechanical properties of TPS. TPS pellets were prepared by using a twin screw extruder with a screw speed of 100 rpm and temperature profile of 70-110-120-120 °C when glycerol was used as a plasticizer, while the screw speed of 20 rpm and temperature profile of 70-110-130-130 °C when a mixture of urea and formamide was used as a plasticizer. TPS pellets were fed into a blown film extruder line (L/D = 25) with a temperature profile of 100-110-120-120 °C. The best material suitable for the film blowing process was based on high-amylose maize starch thermoplasticized with 30% of urea/formamide. Bubbles prepared using this formulation were not sticky and their wall/layer could be separated after calendering. Moreover, no migration of plasticizers and foaming were observed. They also reported that the combination of high-amylose (>51%) starch and urea/formamide mixtures as plasticizer could produce homogenous film of 50 μm thickness and a robust film blowing process due to the good elongational viscosity, high deformability of the melt and strain-hardening behavior.

Mościcki *et al.* (2012) studied the effect of blown film extrusion parameters on the properties of the extrusion-cooked potato starch–glycerol mixtures. Three different compositions of materials composed of potato starch and glycerol, i.e. 80/20, 78/22, 75/25 –weight basis have been prepared. The components were mixed together in a ribbon mixer, followed by blended through an extrusion–cooking process. The obtained TPS was further converted into a film by blown film extrusion conducted on a single screw plastic extruder (L/D = 35) using a screw rotational speed of 90 rpm and temperature range of 70–155 °C. During the blowing, the material was not fully processed and some residual pellets appeared at the film surface, when an

extrusion temperature below 120 °C was applied. The obtained films were thick and opaque, and after storage the film lost its flexibility and became brittle due to its drying up. The films with good quality was obtained when high temperature and screw with additional mixing elements were used. They were flexible, semi-transparent and easy to blow. The best result was reported when the film was extruded from the mixture with 22% of glycerol at a temperature range of 110–140 °C and a screw speed of 90 rpm. However, the authors suggested that mechanical properties of the films were not satisfactory yet in many aspects and needed the incorporation of other components to achieve fully biodegradable packaging materials of good quality.

Apart from blown film extrusion of pure TPS, many research works have reported about blown film extrusion of TPS blended/mixed with other polymers such as PLA (Shirai *et al.*, 2013b), proteins (Zasypkin *et al.*, 1992) and chitosan (Pelissari *et al.*, 2009; Pelissari *et al.*, 2012; Pelissari *et al.*, 2011). The aims of blending were to improve mechanical and barrier properties of the native TPS and also to reduce the cost of the products based on other polymers.

Recently, the growing environmental awareness imposed to packaging films and processes in both user-friendly and eco-friendly attributes. As a consequence bio-based material demands have been growing up so fast because of their advantages such as non-toxicity, completely renewability, biodegradability and compostability. However, there are some problems associated with bio-based polymers such as performances, processing and cost. Therefore, blending/mixing bio-based materials together can not only overcome their disadvantages but also retain their advantages.

Shirai *et al.* (2013a) studied the effects of extrusion process and PLA addition on properties of thermoplastic starch and polyester films by using blown film extrusion. Their results showed that incorporating PLA could increase the elastic modulus, tensile strength, and viscoelastic parameters of the films. The film with 20% of PLA exhibited low WVP due to the hydrophobic nature of this polymer. In another study, Pelissari *et al.* (2012) aimed to improve tensile and water vapor barrier

properties of cassava starch-chitosan blown films by adding low concentration of chitosan flake. They found that the presence of a higher relative concentration of chitosan favored the formation of more rigid and opaque and less permeable films.

2. Chitosan

Chitosan is a natural cationic polysaccharide derived from chitin, which is found in the crustacean shells, insect cuticles and cell walls of fungi. When the degree of deacetylation (DD) of chitin reaches about 70% (depending on the origin of the polymer), it becomes chitosan, a linear polysaccharide consisting of (1,4)-linked 2-amino-deoxy–β–d-glucan (Brück *et al.*, 2010) (Figure 4). There are 3 forms of chitosan, i.e. α, β and γ based on their crystalline structure. β-chitosan chains are arranged in a parallel arrangement with relatively weak intermolecular forces and loose packing, while the α-structure is aligned in an antiparallel fashion responsible for a stronger intermolecular hydrogen bonding (Chen and Zhao, 2012).

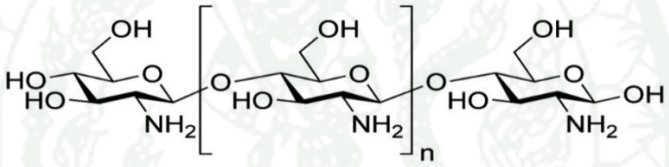

Figure 4 Chemical structure of chitosan.

Properties of chitosan are depended on the degree of deacetylation and its molecular weight. DD determines the content of free amino groups in the polysaccharide; the higher DD corresponds to the greater amount of amino groups. Commercial chitosan usually has a value of DD over 70%. In this manner, it is important to know DD, in order to evaluate the properties of the material including its solubility and further chemical modifications. Therefore, chitosan sample may present different characteristics. The source of chitin and its characteristics directly influence the velocity of the deacetylation reaction. Deacetylation and molecular weight of chitosan also affects mechanical, water vapor barrier and antibacterial properties of the polymer. With high molecular weight, chitosan shows good mechanical and thermal properties. However, molecular weight of chitosan did not influence water vapor permeability (Chen and Zhao, 2012). On the other hand, different molecular weight showed different antimicrobial activities against microorganisms. For example, chitosan with a molecular weight of 746 KDa showed effective antimicrobial activities

against *E.coli* and *P.fluorescens*, while chitosan with a molecular weight of 470 kDa exhibited more effective antioxidant properties against *S.typhimurium* and *V.parahoemolyticus*. Therefore, chitosan with different molecular weight is used for different purposes.

Chitosan is insoluble in water, alkali and organic solvents, but soluble in most solutions of organic acids when the pH of the solution is less than 6. Aqueous acetic and formic acids are two of the most widely used solvents for dissolving chitosan. Some dilute inorganic acids, such as nitric acid, hydrochloric acid, perchloric acid, and phosphoric acid, can also be used to prepare chitosan solution, but only after prolonged stirring and warming because chitosan is a strong base as it possesses primary amino groups with a pKa value of 6.3 (Li *et al.*, 1996; Pillai *et al.*, 2009). The presence of the amino groups indicates that pH substantially alters the charged state and properties of chitosan. At low pH, these amines get protonated by protonation of the –NH2 functional groups on the C-2 position of the D-glucosamine repeat units and become positively charged and that makes chitosan a water-soluble cationic polyelectrolyte. On the other hand, as the pH increases above 6, chitosan's amines were deprotonated and the polymer loses its charge and becomes insoluble.

Beside biodegradability (Dean *et al.*, 2013) and biocompatibility (Richardson *et al.*, 1999), non-toxicity (Kean and Thanou, 2010), antibacterial activity is also one of the most important properties of chitosan. Chitosan has been demonstrated its capability against fungi both Gram-positive and Gram–negative bacteria (Martínez-Camacho *et al.*, 2010; Rodríguez-Núñez *et al.*, 2012). Martínez-Camacho *et al.* (2010) explained antimicrobial activities of chitosan through three mechanisms. Firstly, the positive charges presented on the polymeric chain of chitosan, due to its amino groups, interact with the negative charges from the residues of macromolecules in the membrane of microbial cells, interfering the nutrient exchange between the exterior and the interior of the cells. Secondly, chitosan acts as a chelating agent, creating compounds from traces of metals essential to the cells. Thirdly, chitosan with low molecular weight is capable of entering the cell's nucleus, interacting with the DNA, interfering with the messenger RNA synthesis, affecting the synthesis of proteins and inhibiting the action of various enzymes.

Thus, chitosan can be used in many areas such as biomedical (Dodane and Vilivalam, 1998), cosmetology (Anchisi *et al.*, 2006), waste water treatment (Zeng *et al.*, 2008), agriculture (El-Sawy *et al.*, 2010) and food industries (Dutta *et al.*, 2009). Particularly, its application is also wide range in packaging industries; chitosan can be used as a main raw material for preparing coating film (Bangyekan *et al.*, 2006; Vargas *et al.*, 2006) and solution cast film (Cissé *et al.*, 2012; Giovino *et al.*, 2012) as well as an additive for other polymeric materials to improve their properties (Pelissari *et al.*, 2009; Pelissari *et al.*, 2012; Pelissari *et al.*, 2011). Recently, a number of research studies involved blown film extrusion of some thermoplastic polymers such as PLA (Bonilla *et al.*, 2013c) and thermoplastic starch (Pelissari *et al.*, 2012) with chitosan additive have been received much attention because this technique can be transferred to the conventional plastic industries and it is an effective way to add value of chitosan, a solid waste from seafood industry. Nevertheless, chitosan cannot be melt and homogeneously blended with other thermoplastic materials during extrusion process, its remnants still dispersed in the film matrix (Bonilla *et al.*, 2013c).

Therefore, the present thesis focuses on the preparation of homogeneous thermoplastic starch/chitosan-based film using blown film extrusion and also studies the effect of chitosan on blown film extrusion processability, characteristics and properties of thermoplastic starch film.

3. Starch/chitosan-based films

There are two techniques used to prepare starch/chitosan-based films, i.e. solution casting method and blown film extrusion. From the literatures, although most of starch-based films including starch/chitosan films have been prepared by a solution casting method, this technique is quite taking longer time and low productivity efficiency. Blown film extrusion technology has become an attractive option to produce starch-based films in the form of thermoplastic, due to its high productivity efficiency, which is suitable for industry.

Several studies have revealed the preparation and properties of starch/chitosan-based films obtained from solution casting process. Examples are as follows:

Xu *et al.* (2005) prepared chitosan/starch composite films by combining chitosan solution (deacetylated degree of 90%) and two thermally gelatinized corn starches (waxy starch and regular starch with 25% amylose). Chitosan solution and starch solution were mixed before cast onto a glass plate at room temperature for at least 72 h. The chitosan/starch ratio was varied as 0.5:1, 1:1, 1.5:1 and 2:1. Dried films were conditioned at 25 °C, 50% RH for 48 h. Glycerol was added as 25% (w/w) of the total solid weight in solution. The authors mentioned that the films made only from chitosan lacked of water resistance and have poor mechanical properties. The results showed that the amino group band of chitosan molecule in the FTIR spectrum shifted from 1578 cm^{-1} in the chitosan films to 1584 cm^{-1} in the composite films, indicating a molecular miscibility between these two components. In case of mechanical properties, composite films prepared using regular starch showed higher tensile properties as well as elongation at break than those obtained from waxy starch. In addition, the highest values of both tensile strength and elongation were obtained for the composite films composed of chitosan and starch with the weight ratio of 1:1. The decrease in tensile strength and elongation at other weight ratios might be due to the formation of intra-molecular hydrogen bonds rather than inter-molecular hydrogen bonds, resulting in a phase separation between the two main components.

Bourtoom and Chinnan (2008) prepared biodegradable blend films from rice starch and chitosan by a solution casting method. Starch and chitosan solutions were blended using a weight ratio of starch:chitosan of 2:1, 1.5:1, 1:1 and 0.5:1. The mixtures were cast onto non-stick trays at 55 °C for 10 h and then stored in plastic bags and held in desiccators at 60% RH. Commercial grade chitosan flake with approximately 85% DD and molecular weight of about 75 kDa was used. Sorbitol was added about 40% (w/w) of total solid weight in solution as a plasticizer. The introduction of chitosan resulted in increased tensile strength, water vapor permeability, lighter color and yellowness, but decreased elongation at break and solubility of the biodegradable blend films. Other results from XRD showed that the incorporation of chitosan increased the crystalline peak intensity of starch film, however, too high chitosan concentration yielded phase separation between starch and chitosan. The amino group band of the chitosan molecule in the FTIR spectrum shifted from 1541.15 cm^{-1} in the chitosan film to 1621.96 cm^{-1} in the blend film. These results indicated that

there was a molecular miscibility between these two components. In addition, the authors also compared the properties of rice starch–chitosan blend film, selected biopolymer with those of synthetic polymer films. The results demonstrated that mechanical properties of rice starch–chitosan blend film were similar to those of other chitosan films; however the blend film possessed higher tensile strength but lower elongation at break than some synthetic polymers (LDPE and HDPE). In addition, the water vapor permeability of rice starch–chitosan biodegradable blend film was relatively lower than that of chitosan films, but higher than that of polyolefin.

Chillo *et al.* (2008) investigated the influence of glycerol and chitosan on tapioca starch–based edible film using response surface methodology. Glycerol and chitosan concentrations were varied in the range of 0.5%–1.25% (w/w) and 0.1%–1% (w/w), respectively. Concentration of tapioca starch was maintained at 2% for all blend solution. Edible films were obtained by a casting technique at 32 °C for 48 h and the films were stored in plastic bags and held in desiccators at 25 °C, 57.5% RH. Incorporating chitosan could improve mechanical properties of starch–based film, while adding glycerol showed opposite results. With regard to WVP data, the addition of chitosan had a negative effect, whereas that of glycerol had a positive influence to WVP values. The authors explained about the permeability increment and the plasticizing effect of glycerol, which reduce polymeric chain packing density. In addition, the increase of hydrogen bonding interactions between chitosan and tapioca starch reduces the hydrophilic group availability, therefore reducing the water vapor transmission rate. Both chitosan and glycerol influenced the color indices.

Bonilla *et al.* (2013a) evaluated the effect of chitosan on the physical properties of wheat starch-glycerol films. Solution casting process was used to prepare the films and the effect of film composition on their properties was studied. Starch and chitosan solutions were mixed by using a ratio of starch:chitosan of 100:0, 90:10, 80:20, 70:30, 60:40, 50:50 and 0:100. Films were obtained by drying the mixture at room temperature, 60% RH and then conditioned at 5 °C, 58% RH. The combined effect of the glycerol and chitosan proportions on mechanical and barrier properties of the films was studied. Tensile strength and elastic modulus of the films increased with increasing chitosan concentration due to increased cooperative van der Walls forces in the matrix

as a consequence of its greater capacity to form hydrogen bonds. In addition, oxygen and water vapor permeability of the film slightly increased with the amount of chitosan in the blend. Chitosan concentration directly affected the antimicrobial properties of the films; the film with a chitosan–starch ratio of 50% showed a significant antibacterial activity.

From the above articles, most studies are relevant to the influence of chitosan on the properties of starch-based films produced only by the solvent casting method. Although they proved that the addition of chitosan could improve mechanical and water vapor barrier properties of starch-based films as well as impart antimicrobial activity to the films; the fabrication of starch-based films using solution casting method is not useful enough to apply in the industrial level due to the limited productivity. Blown film extrusion is an alternative option to approach the industrial goal. Only few publications have been mentioned about applying blown film extrusion process to develop starch/chitosan-based films (Pelissari *et al*., 2009; Pelissari *et al*., 2011; Pelissari *et al*., 2012).

Pelissari *et al.* (2009) studied the antimicrobial, mechanical and barrier properties of cassava starch/chitosan films incorporated with oregano essential oil (OEO). The films were produced by using a single screw extruder. The extrusion was performed twice, i.e. for producing the pellets and fabricating the tubular films. In the first stage of the extrusion process, the mixtures of starch, chitosan and glycerol were extruded with a temperature profile of 120/120/120/110 °C and a screw speed of 35 rpm. The OEO was added to the pellets, which were reprocessed. Next, the preprocessed pellets were extruded again to form film via blown film extrusion using a temperature profile of 120/120/120/120/130 °C and a screw speed of 35 rpm. Concentrations of starch was varied in the range of 77%–82% (w/w) and concentrations of chitosan used was 5% (w/w). Glycerol concentration was maintained at 18% and OEO was also varied in the range of 0.1–1 g. The antimicrobial effect of starch/chitosan/OEO films against *Bacilus cereus, Escherichia coli, Salmonella enteritidis,* and *Staphylococcus aureus* was determined by a disk inhibition zone assay. The results suggested that chitosan was not effective against the tested organisms, but it

reduced rigidity and water vapor permeability of the film. TGA analysis demonstrated that the addition of chitosan did not affect the thermal stability of the films.

Two years later, Pelissari *et al.* (2011) reported the effect of extrusion parameters on the properties of starch/chitosan active film. The extrusion temperature (120, 130 and 140 °C) and screw speed (25, 35 and 45 rpm) were two parameters that they studied. Based on the formulation of the active film prepared in their previous paper, the proportion of starch of 77% (w/w), chitosan of 5% (w/w), and glycerol of 18% was selected to be studied in this work because this formulation had the best mechanical properties. A concentration of OEO of 0.5% in relation to total basic formulation was added. The increase in screw speed had a positive effect on blow-up ratio and water vapor permeability but a negative effect on opacity, tensile strength and elongation at break of the films. Using low die temperatures resulted in decreased tensile strength, elongation at break, Young's modulus and water vapor permeability of the films. On the other hand, sorption isotherms of the films were directly influenced by the extrusion conditions. The films produced at 130 °C and 35 rpm were less hydrophilic.

In 2012, Pelissari *et al.* revealed the constrained mixture design applied to improve the mechanical properties and water vapor permeability of cassava starch/chitosan blown films. The mixture of starch, chitosan and glycerol was extruded and pelletized twice to obtain a good homogenization using a barrel temperature profile of 120/120/120/110 °C and a screw speed of 35 rpm. The pellets were then used to manufacture the film by blown film extrusion with a temperature profile of 120/120/120/120/130 °C and same screw speed as the compounding step. The concentrations of starch, chitosan and glycerol were varied in the ranges of 72.5%–82%, 2.5–5%, 18-25%, respectively. According to the models generated by the design, the concentration of starch had a positive effect in both mechanical and water barrier properties. The glycerol plasticizer and its interactions with other components had a positive effect on increasing the water vapor permeability. On the other hand, the presence of a higher relative concentration of chitosan favored the formation of more rigid and opaque and less permeable films.

Although chitosan has been incorporated into thermoplastic starch films using an extrusion technology, it was in a flake form which caused film surface roughness (Bonilla *et al.*, 2013c). Therefore, the present thesis studies the loading of chitosan in the form of solution (in aqueous acetic acid) into TPS film by blown film extrusion. In this case, we e expected that crystallinity of chitosan would be destroyed before passing through a twin-screw extruder, in which TPS was fabricated, to provide homogeneous materials of TPS and chitosan resulting in enhanced processability and blown film properties. In addition, the effect of chitosan on blown film extrusion processability, characteristics and properties of the films was also investigated.

MATERIALS AND METHODS

Materials

1. Materials

1.1 Native cassava starch (moisture content = 11%) (Dragon Fish brand, Tong Chan Registered Ordinary Partnership, Thailand)

1.2 Glycerol (commercial grade)

1.3 Chitosan (deacetylation degree = 0.85 and molecular weight = 500,000 Da) (Seafresh Chitosan (Lab) Co., Ltd., Thailand)

1.4 Acetic acid (99%) (Merck, Germany)

1.5 Ninhydrin (Loughborough, UK)

1.6 Sodium acetate (Ajax Finechem, Australia)

1.7 Dimethylformamide (ACI Labscan, Thailand)

2. Equipment and glasswares

2.1 Magnetic bars

2.2 Beakers

2.3 Plastic trays

2.4 Graduated cylinders

2.5 Micrometer (ID-C112BS, Mitutoyo, Japan)

2.6 Cups for WVTR measurement

3. Machines

3.1 Twin-screw extruder (L/D = 40 and screw diameter = 20 mm) (LTE-20-40, Labtech Engineering Co., Ltd., Thailand)

3.2 Single-screw extruder (L/D = 30 and screw diameter = 25 mm) (LE-25-30/C, Labtech Engineering Co., Ltd., Thailand,) with a film-blowing attachment (LF-400, Labtech Engineering Co., Ltd., Thailand)

3.3 Pelletizer (LZ-120, Labtech Engineering Co., Ltd., Thailand)

3.4 Hot air oven (FD 53, Scientific promotion Co., Ltd., Thailand)

3.5 Differential scanning calorimeter (DSC822, Mettler Toledo, Switzerland)

3.6 Thermogravimetric analyzer (STA PT1000TG, Linseis, Germany)

3.7 Instron test machine (5965, Instron, UK)

3.8 Oxygen permeation analyzer (Model 8501, Illinois, USA)

3.9 Melt flow indexer (MFI-203, Custom Scientific, USA)

3.10 UV-Visco spectrophotometer (UV-2450, Shimadzu, Japan)

3.11 Incubator (KBF 240, Scientific Industries, USA) for WVTR measurement

3.12 X-ray diffractomer (JDX- 3530, JEOL, Japan)

3.13 Scanning electron microscope (JSM -6610lv, JEOL, Japan)

3.14 Fourier transform infrared spectrometer (Tensor 27 FTIR, Bruker Corporation, Germany)

3.15 Contact angle analyzer (OCA 15EC, DataPhysics Instruments GmbH, Germany)

3.16 Dynamic mechanical thermal analyzer (EPLEXOR 150N, GABO qualimeter, Germany)

Methods

1. Preparation of thermoplastic starch/chitosan compounds by extrusion

Chitosan solution (w/v) was prepared by dissolving chitosan flakes (0.5, 1, 1.5, 2 part(s) per hundred parts of starch (phs)) in an aqueous acetic acid solution (1% v/v, 100 mL) with supporting of magnetic stirrer at 550 rpm until the dissolution was completed, which typically taking about 48 h at ambient temperature.

Starch, glycerol (35 phs) and chitosan solution were thoroughly mixed by stirring at ambient temperature for 15 min. The slurry was then poured into a plastic tray with 1.5 cm-height volume and stored in a hot air oven at 65 °C for 18 h to get solid material. After that, it was ground into powder with a moisture content approximately of 20-22%, then blended in a twin–screw extruder (L/D = 40, screw diameter = 20 mm, LTE-20-40, Labtech Engineering Co., Ltd., Thailand) using a

barrel temperature profile of hopper/90/95/105/110/115/120/120/120/120/125 °C/die and screw speed of 170 rpm. The extrudates were cut into pellets with a pelletizer to have a length of 2 mm. Four formulations of thermoplastic starch/chitosan compounds, i.e. TPS/CTS0.5, TPS/CTS1, TPS/CTS1.5 and TPS/CTS2 representing thermoplastic starch containing chitosan with a content of 0.5, 1, 1.5 and 2 phs, respectively, were obtained. TPS without addition of chitosan was also prepared and used as a control.

2. Preparation of thermoplastic starch/chitosan films by blown film extrusion

The obtained pellets were blown into a film by using a single-screw extruder (L/D = 30, screw diameter = 25 mm, LE-25-30/C, Labtech Engineering Co., Ltd., Thailand) with a film-blowing attachment (LF-400, Labtech Engineering Co., Ltd., Thailand), and four controlled temperature zones connected to a ring-shaped die. The barrel temperature profile was maintained at: feed inlet/130/140/140/140 °C/die and the die temperature was set at 150/150 °C. Screw speed and nip roll speed were adjusted to be 35–45 rpm and 3 rpm, respectively. The control film was prepared using the same method, but without adding chitosan. The obtained films were stored inside the zip lock PE bags containing silica gel at ambient temperature (42 ± 2 %RH) to avoid moisture absorption.

3. Characterization and properties testing of thermoplastic starch/chitosan films

3.1 Melt flow index measurement

Melt flow index (MFI) of the samples was measured according to ASTM 1238-10 with a slight modification. The measurement was performed using an MFI-203 (Custom Scientific, USA) at 190 °C with a load cell of 3.2 kg, a time interval of 6 min and a preheating time of 7 min. MFI was measured in triplicate and reported as a mean ± SD in g/10 min.

3.2 Measurement of UV absorption and transparency

UV absorption and light transmittance of the films were measured at the wavelength ranges from 200 nm to 400 nm and from 400 nm to 800 nm, respectively, using a UV-2450 Ultraviolet-Visible (UV-Vis) spectrophotometer (Shimadzu, Japan).

3.3 Fourier transform infrared analysis

Fourier transform infrared (FT-IR) spectra of samples were recorded with an attenuated total reflectance (ATR) mode using a Bruker Tensor 27 FTIR spectrometer (Bruker Corporation, Germany). The spectra were recorded from 500 cm^{-1} to 4000 cm^{-1} at different temperatures varying from 30 °C to 220 °C using accumulated scans of 32 and spectral resolution of 4 cm^{-1}.

3.4 X-ray diffraction analysis

X-ray diffraction (XRD) patterns of the samples were analyzed by a JEOL JDX–3530 X-ray diffractomer (JEOL, Japan). Sample was scanned at the diffraction angel (2θ) of 5–40° using a scan rate of 0.02°/sec.

3.5 Thermogravimetric analysis

TGA themogram was obtained using a STA PT1000TG (Linseis, Germany), with a TA evaluation software. Sample (15–25 mg) was put in a crucible and then heated up from 25 °C to 600 °C under nitrogen atmosphere using a N_2 flow rate of 4 L/h and a heating rate of 20 °C/min.

3.6 Dynamic mechanical thermal analysis

Dynamic mechanical thermal analysis (DMTA) was performed by an EPLEXOR® DMA (GABO qualimeter, Germany) in the tension mode at a frequency of 1.5 Hz, static load of 0.5 N and dynamic load of 0.15N. Scanning temperature was ranged from -80 °C to 55 °C with a heating rate of 3 °C/min. Sample was cut into rectangular shape with a dimension of 10 mm × 50 mm. The grips was used to hold sample firmly without an excessive deformation before test. Storage modulus (E')

and tan delta (tanδ) were evaluated for each sample. Three repetition were tested for each sample.

3.7 Differential scanning calorimetric analysis

Differential scanning calorimetric (DSC) analysis was carried out using a DSC822e differential scanning calorimeter (Mettler Toledo, Switzerland). Sample (10–15 mg) was packed in an aluminum pan and then sealed up a lid. The DSC analysis was accomplished under nitrogen atmosphere with a N_2 flow rate of 50 mL/min. The first heating scan was performed from 0 °C to 250 °C with a heating rate of 5 °C/min, then cooled down to 0 °C with a cooling rate of 5 °C/min, followed by heating up again from 0 °C to 250 °C with a heating rate of 5 °C/min.

3.8 Tensile testing

Tensile properties of the sample films were tested using a 5965 universal testing machine (Instron, USA) according to the standard method D882–12 (ASTM, 2012) with a modified storage conditions. Samples were cut into rectangular shape with a dimension of 3 cm × 15 cm and then conditioned at ambient temperature with % RH of 62 ± 2 and 42 ± 2 for at least two days prior to test. Five specimens were tested for each sample. Thickness of the sample films was measured by an ID-C112BS micrometer (Mitutoyo, Japan) with an accuracy of 0.0001 mm. The average thickness of each film was measured from 5 points of each specimen. Tensile strength (MPa), modulus of elasticity (MPa) and elongation at break (%) were recorded as a mean ± SD. The initial grip distance was set at 100 mm and the crosshead speed was 50 mm/min.

3.9 Morphological observation by scanning electron microscope

The sample films were placed on the stub using a two-sided carbon tape and then coated with a thin layer of gold. Morphology of the films was observed using a JSM-6610lv (JEOL, USA) at an accelerating voltage of 20 kV.

3.10 Investigation of the presence of chitosan on the film surface by reaction with ninhydrin

The presence of chitosan on the film surface was investigated by complex formation with ninhydrin. Acetate buffer (pH 5.5, 5 mL) and freshly prepared ninhydrin reagent (50 mg/mL of ninhydrin in dimethyl formamide, 40 mL) were mixed together. 10 μL of ninhydrin solution was dropped on the films surface, then heated up for 30 sec. After that, the color of the films was observed.

3.11 Determination of water vapor permeability

Water vapor transmission rate (WVTR) of the films was determined according to ASTM E96. Sample film was cut into circle shape with a diameter of 7.5 cm and then placed on the open mouth of a test cup, which has an inner diameter of 6.3 cm and contained dried desiccant (20 mL). The film was sealed to the cup using paraffin wax. The sample assemblies were weighed before placing in an incubator at 25 °C and 50% RH. Each sample was periodically taken out and weighed until its constant weight was obtained. Three specimens were tested for each sample. WVTR was determined as a slope of the linear portion of a plot of weight gained versus time (g/day) divided by the sample permeation area (m^2). Steady state over time (slope) yielded a regression coefficient of 0.99 or greater. The water vapor permeability (WVP) was calculated from Eq. 1.

$$WVP = (WVTR \times L)/ \triangle P \qquad (1)$$

Where WVP is the water vapor permeability ($g.mm/m^2.hr.atm$), WVTR is the water vapor transmission rate through a film ($g/m^2.hr$), L is the mean film thickness (mm) and ΔP is the partial water vapor pressure difference between the two sides of the film (atm). The results were recorded as mean ± SD.

3.12 Water contact angle measurement

Water contact angle was measured by an OCA 15EC contact angle analyzer (DataPhysics Instruments GmbH, Germany) using an SCA 20 software to analyze the data. Sample film was cut into a rectangular shape (1 cm × 5 cm) and then immobilized on a stand. A drop of distilled water (3 μL) was placed on the film before measurement. Three repetition was performed for each sample.

3.13 Determination of oxygen permeability

Oxygen transmission rate (OTR) of the films was determined in accordance with the ASTM D3985 using an lllinois 8000 oxygen permeation tester (Illinois Instruments Inc., USA). The film was cut into a circle shape with a diameter of 14 cm and conditioned in desiccator containing saturated calcium chloride solution for at least 48 h. Three specimens were tested for each sample. Oxygen permeability (OP) was calculated by using Eq. 2.

$$OP = (OTR \times L)/\Delta P \qquad (2)$$

Where OP is the oxygen permeability (cc.mm/m^2.day.atm). OTR is the oxygen transmission rate through a film (cc/m^2.day), L is the mean thickness (mm) and ΔP is the oxygen partial pressure difference between the two sides of the film (atm). The results were recorded as mean ± SD.

3.14 Statistical analysis

Statistical differences of the data were analyzed by the analysis of variance (ANOVA). Duncan's multiple range test ($p < 0.05$) was used to evaluate differences among mean values of each sample. Statistical analysis was conducted with an SPSS 11.0 for windows.

RESULTS AND DISCUSSION

1. Melt flow ability of thermoplastic starch/chitosan compounds

Four formulations of thermoplastic starch/chitosan compounds, i.e. TPS/CTS0.5, TPS/CTS1, TPS/CTS1.5 and TPS/CTS2 representing thermoplastic starch containing chitosan with a content of 0.5, 1, 1.5 and 2 phs, respectively, were prepared. TPS without addition of chitosan was used as a control.

The melt flow behavior at low shear force of TPS and TPS/CTS compounds was relevant to the value of melt flow index (MFI). High MFI value indicates good flow, small molecules and low melt viscosity.

MFI of TPS/CTS compounds was measured according to ASTM 1238-10; however it could not be determined using the load of 2.16 kg due to an extremely high melt viscosity. Therefore, the load cell of 3.2 kg was applied for this experiment. MFI value of TPS was about 1.32 g/10 min, while those of TPS/CTS compounds varied from 0.09 g/10 min to 0.81 g/10 min (Fig. 5). The result showed that melt flow ability of TPS decreased by incorporating chitosan. In addition, melt flow ability significantly decreased with increasing chitosan content, such as about three times for TPS/CTS1 as compared with TPS/CTS0.5. This result might come from the interaction between starch and chitosan molecules via hydrogen bond formation leading to decreased melt flow ability of the materials when chitosan content increased.

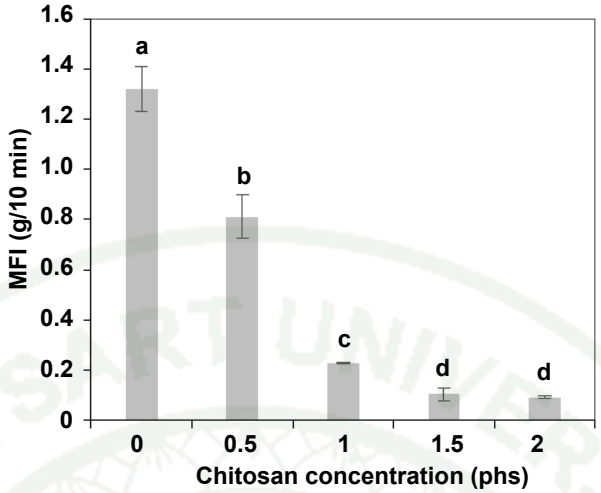

Figure 5 Melt flow index of TPS and TPS/CTS compounds containing different chitosan concentrations. The data is reported as mean ± SD, *n = 3*. The different small letters indicate significant difference at $p < 0.05$ (Duncan's new multiple range test).

2. Color, UV absorption and transparency of thermoplastic starch/chitosan films

Color and transparency of packaging film are important in terms of general appearance, consumer acceptance and utilization. Fig. 6A shows that L^* value of TPS/CTS films was lower than that of TPS film and the L^* value of TPS/CTS films significantly decreased with increasing chitosan concentration. This result implied that the presence of chitosan caused the darker film. TPS film showed slightly increased a^* value and markedly increased b^* value when chitosan was incorporated. However, the film color still be in yellow-red shade since a^* and b* values are positive. The values of a^* and b^* of TPS/CTS films tended to increase with increasing chitosan content. The results suggested that the films became more intense yellow.

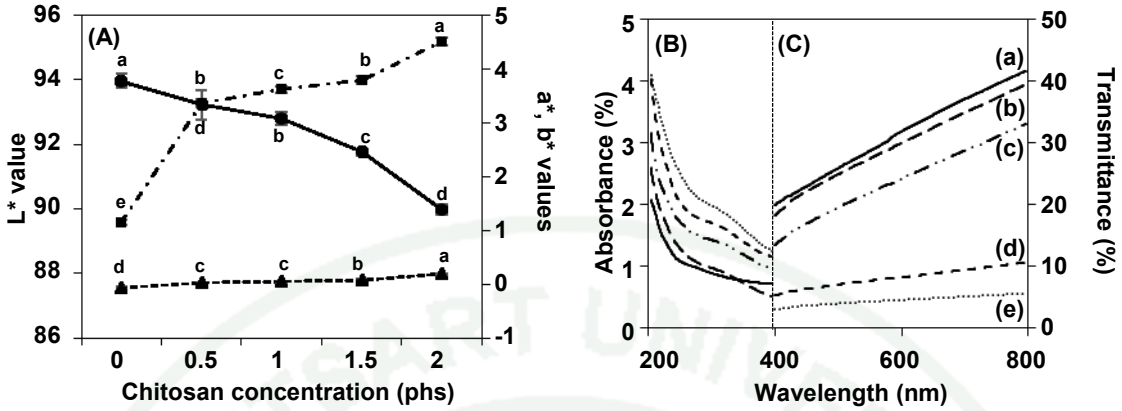

Figure 6 (A) Color parameters: L^* (●), a^* (▲) and b^* (■), (B) UV absorbance and (C) transparency of different sample films: (a) TPS, (b) TPS/CTS0.5, (c) TPS/CTS1, (d) TPS/CTS1.5 and (e) TPS/CTS2. For (A), the data is reported as mean ± SD, $n = 3$. The different small letters indicate significant difference at $p < 0.05$ (Duncan's new multiple range test).

UV absorption of the sample films was measured at the wavelength ranged from 200 nm to 400 nm. TPS/CTS films showed higher UV absorption than TPS film and UV absorption of the TPS/CTS film increased with increasing chitosan content (Fig. 6B). The result suggested that chitosan could impart UV light protection to TPS film. This might be useful for the film to retard lipid oxidation induced by UV light. Bonilla *et al.* (2013c) also reported that PLA/CTS films showed higher absorbance in the wavelength range of 200-400 nm than naked PLA film suggesting better barrier to ultraviolet light.

Transparency of the sample films was determined from the light transmission at selected wavelengths from 400 nm to 800 nm. The transmittance values of all samples increased with increasing wavelength (Fig. 6C). TPS/CTS films showed lower light transmittance values than TPS film, indicating that the films became more translucent or opaque by adding chitosan. The higher chitosan contents gave more opacity of the films. This might be explained by the highly dispersed chitosan in TPS/CTS matrix.

3. Chemical interaction of thermoplastic starch/chitosan films

FITR spectroscopy was used to examine the chemical interaction between starch and chitosan. TPS film exhibited characteristic bands at 3297 cm^{-1} (OH stretching), 2928 cm^{-1} (C–H stretching), 1640 cm^{-1} (δ(O–H) bending of water), 1365 cm^{-1} (CH_2), 1015 cm^{-1} (C–O–C bond stretching) and 926 cm^{-1} (pyranose ring) (Delval *et al.*, 2004) (Fig. 7Aa). All TPS/CTS films showed similar FTIR spectra (Fig. 7Ab-e) to TPS film because chitosan chemical structure is similar to that of starch. It should be pointed out that amide I and amide II bands of chitosan were not observed in the spectra of TPS/CTS films due to the extremely small amount of chitosan added. Hydrogen bond between starch and chitosan molecules was expected to be possible interaction in this TPS/CTS system. Fig. 7A also shows that OH band of starch was shifted to higher wavenumber when chitosan was added, implying that hydrogen bonds between starch molecules became weak because some of them formed intermolecular hydrogen bond with chitosan. However hydrogen bond interaction was difficult to identify from the spectra characterized at ambient temperature due to the effect of moisture. Skrovanek *et al.* (1985) reported that the destruction of hydrogen bond could be observed at high temperature. Herein, we analyzed FTIR of the sample at various temperatures from 30 °C to 220 °C. Fig. 7B shows that OH band of both TPS and TPS/CTS films became broader with lower intensity when temperature increased. In addition, the OH band was shifted to higher frequency with increasing temperature. The results implied that increasing temperature caused the reduction of the average strength of the hydrogen bonds and a broadening of the distribution (Eichhorn *et al.*, 2003; Kössler *et al.*, 1990). Eichhorn *et al.* (2003) studied temperature-dependent FTIR spectroscopy of hydrogen bonding of pentadecyl phenol and reported that during heating the sample up to 150 °C, the hydrogen-bonded hydroxyls shifted to higher wavenumber and the bands became broader. In addition, TPS/CTS film showed higher degree of OH band shift than TPS film (Fig. 7B), indicating that hydrogen bonds between starch molecules became more weaker when chitosan was incorporated because chitosan could form hydrogen bond interaction with starch molecules.

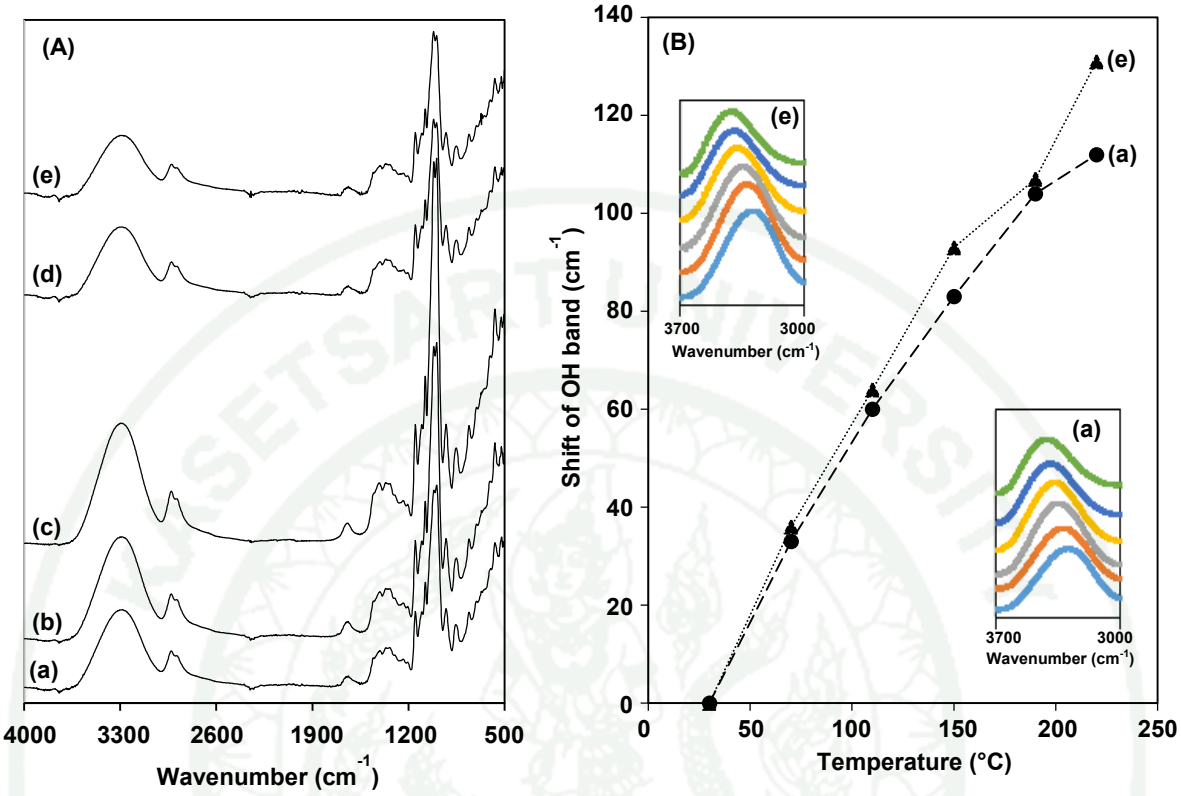

Figure 7 (A) FTIR spectra and (B) shift of OH band of different sample films: (a) TPS, (b) TPS/CTS0.5, (c) TPS/CTS1, (d) TPS/CTS1.5 and (e) TPS/CTS2. Inset of (B) represents FTIR spectra as a function of temperature: from bottom to top, 30 °C, 70 °C, 110 °C, 150 °C, 190 °C and 220 °C.

4. Crystal structure of starch in thermoplastic starch/chitosan films

Crystal type of starch in the film samples was analyzed by XRD technique. TPS film showed the characteristic diffraction peaks at 2θ of 13.1°, 18.2°, 19.6° and 24° (Fig. 8a). The peaks at 2θ of 13.1° and 19.6° were ascribed to V_H-type crystal formed by complexation of amylose and glycerol (Shi *et al.*, 2007), whereas the peaks at 2θ of 18° and 24° belonged to B-type crystal (Bangyekan *et al.*, 2006), which might take place during storage. A higher humidity or higher water uptake as well as higher temperature (particularly than T_g) speeds up the B-type crystal formation due to high mobility of the starch polymeric chains. Rindlav-Westling *et al.* (1998) revealed that

an increased air humidity during film formation leaded to longer time contact with water and resulted in high mobility of the starch polymer chains, caused increased B-type crystallinity. V-type crystal bands became broader with increasing chitosan content, implying that the number of amylose-glycerol complexes decreased due to the limited amylose mobility, since it formed hydrogen bond interaction with chitosan. Zhong *et al.* (2011) also reported that kudzu starch-chitosan composite films had broad amorphous peak as compared with starch film, demonstrating that the intermolecular interactions among the components limited the molecular chain segment movements and restrained the crystallization process.

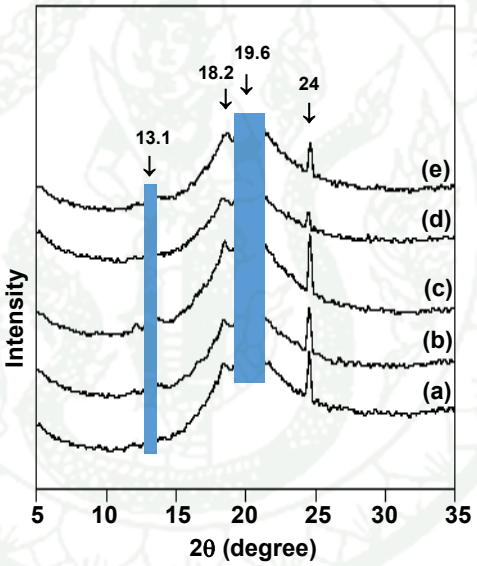

Figure 8 XRD patterns of different sample films: (a) TPS, (b) TPS/CTS0.5, (c) TPS/CTS1, (d) TPS/CTS1.5 and (e) TPS/CTS2.

5. Thermal stability of thermoplastic starch/chitosan films

Thermal stability of TPS and TPS/CTS films was evaluated by TGA technique. TPS film illustrated clearly a three-step weight loss at the temperature ranges of 80-106 °C, 106–200 °C and 200-360 °C attributing to free water evaporation (Pelissari *et al.*, 2009), bound water and glycerol evaporation (Chen *et al.*, 2005), and starch decomposition (Pelissari *et al.*, 2009), respectively (Fig. 9Aa).

However, TPS/CTS films exhibited two-step weight loss at the temperature ranges of 80-240 °C and 240-360 °C belonging to water and glycerol evaporation (Cyras *et al.*, 2008) as well as decomposition of starch and chitosan (Pelissari *et al.*, 2009), respectively (Fig. 9Ab-e). The weight reduction of the film decreased when chitosan was incorporated and it also decreased with increasing chitosan content. For example, total weight loss of TPS film at 250 °C was 20.9%, while those of TPS/CTS films were in the range of 10.6-15.9%. After decomposition (350 °C), the remained weight of TPS film was lowest while those of TPS/CTS films showed higher, implying that TPS/CTS films contained higher amount of inorganic substances. The above results implied that incorporation of chitosan could reduce water absorption and improve thermal stability of TPS film. This might be a result of the hydrogen bond formation between two polymers. However, decomposition temperature of TPS film hardly changed by adding chitosan, i.e. $T_d \approx 300$ °C (Fig. 9B).

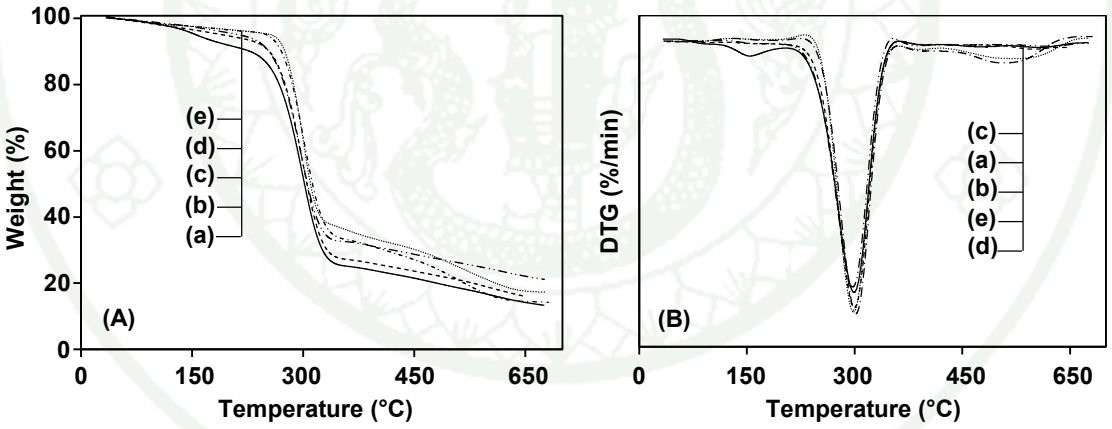

Figure 9 (A) TGA and (B) DTG thermograms of different sample films: (a) TPS, (b) TPS/CTS0.5, (c) TPS/CTS1, (d) TPS/CTS1.5 and (e) TPS/CTS2.

6. Dynamic mechanical thermal properties of thermoplastic starch/chitosan films

Dynamic mechanical thermal properties or phase relaxation behavior of TPS and TPS/CTS films were investigated by DMTA technique at the frequency of 1.5 Hz, static load of 0.5 N and dynamic load of 0.15 N. The obtained storage modulus is

generally relevant to the stored energy, representing the elastic portion of the material, while the loss modulus was used to indicate the energy dissipated as heat, representing the viscous portion. Tan δ (loss factor) is defined as the ratio of loss modulus to storage modulus (Tan δ = E''/E'), where δ is the angle between in-phase and out-phase components of the modulus in the cyclic motion.

Storage modulus of all samples slightly decreased with increasing temperature up to 10 °C and then sharply decreased to 23 °C (Fig. 10A), implying that the materials became soft upon heating. The marked reduction of storage modulus of the latter involved the transition of the materials from glassy to rubbery states. At the temperature below transition point, TPS/CTS films exhibited higher storage modulus than TPS film and the storage modulus of the films increased with increasing chitosan content (Fig. 10A). The result reflected that incorporating chitosan enhanced stiffness and brittleness of TPS film. This could be explained by the lower chain mobility of starch due to its interaction with chitosan.

Glass transition temperature (T_g) of components in TPS and TPS/CTS films could be determined from the highest transition peak of loss factor-temperature curve. Tan δ curves described a partially miscible system with two main relaxations appeared at –50 °C to -40 °C and 16 °C to 22 °C (Fig. 10B). The lower temperature relaxation was attributed to the T_g of the glycerol-rich phase, while the higher temperature relaxation belonged to starch in TPS (Roz *et al.*, 2006). TPS film showed T_g of 16 °C, whereas TPS/CTS films possessed T_g in the range of 19.2-22.1 °C. The results showed that T_g of TPS increased by incorporating chitosan, indicating that the mobility of starch chains in TPS/CTS films was restrained due to the interaction between starch and chitosan. Chang *et al.* (2010) also reported that the glass transition temperature of glycerol plasticized-starch was shifted to higher temperature with the introduction of chitosan nanoparticles due to the formation of composites of glycerol plasticized-starch matrix and chitosan nanoparticles. The nanoparticles improved the intermolecular interaction in the matrix, bringing adjacent chains of starch closer and reducing the free volume.

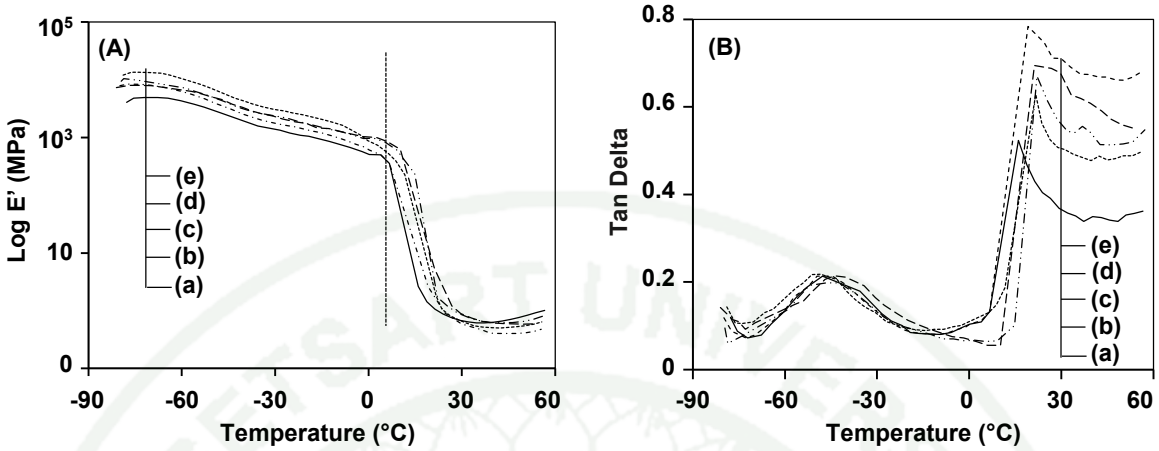

Figure 10 (A) Storage modulus and (B) tan δ of different sample films: (a) TPS, (b) TPS/CTS0.5, (c) TPS/CTS1, (d) TPS/CTS1.5 and (e) TPS/CTS2.

7. Thermal properties of thermoplastic starch/chitosan films

Thermal properties of TPS and TPS/CTS films were analyzed by DSC technique. The heating-cooling cycle was performed twice. From the first heating scan, TPS and TPS/CTS films showed endotherm transitions at the temperature range of 47.2-49.8 °C belonging to glass transition temperature (T_g) of starch, and endothermic peaks at the temperature range of 186-210 °C attributing to melting temperature (T_m) of starch crystal (Fig. 11A). The result suggested that starch existed in both TPS and TPS/CTS films was semi-crystalline polymer after passing through a twin screw extruder and storing at ambient temperature for a certain time. The crystallinity of starch was related to the formation of amylose-glycerol complexes (V-type crystal) (Hulleman *et al.*, 1996; Soest and Essers, 1997) and the assembly of six double helices of glucose residues with hexagonal unit cell containing 36 water molecules inside (B-type crystal) (Imberty and Perez, 1988), which is in agreement with the XRD result. In addition, the enthalpies (△H) or energy used to destroy those crystal structures were in the range of 47- 60 (J/g). However, the films possessed different thermal history after extrusion and also absorbed different content of

moisture during storage; therefore the information from the first heating scan would not be used for comparison study in the present work.

The second heating scan was then performed and its information was compared. T_g of starch in TPS film was 53 °C, while those in TPS/CTS films were in the range of 54-72 °C (Fig. 11B). T_g of starch in the films increased with increasing chitosan content, implying that incorporating chitosan into TPS film caused difficulty in changing the state of starch in TPS from glassy to rubbery ones due to the hydrogen bond formation between starch and chitosan. This result showed the same trend as that obtained from DMTA. However, T_g values obtained from DMTA technique were slightly lower than those derived from DSC technique. The T_g difference is expected in terms of how the structural relaxation of the material responds to thermal and mechanical stimuli. The lower T_g obtained from DMTA might be explained by the application of both heat and mechanical stress, whereas only heat was supplied in DSC measurement. Sakurai *et al.* (2000) reported that the increase of T_g of chitosan/poly(N-vinyl pyrrolidone) blends by increasing chitosan content resulted from a polymer miscibility at molecular level. It should be pointed out that T_m of starch was not observed in the thermogram of second heating scan, reflecting that starch crystal had been completely destroyed at 250 °C (see first heating scan in Fig. 11A) and it could not be reformed during cooling process (no T_c was observed in the thermogram of cooling scan (data not shown)) due to the difficulty of large starch molecules to rearrange themselves in high degree of structural order when relatively fast cooling rate (5 °C/min) was applied. Stagner *et al.* (2011) also reported that thermoplasticized high amylose starch prepared using reactive extrusion did not show endotherm transition in the second heating scan because there was not enough time for crystallization during cooling (10 °C/min), thus no crystallization exotherm or subsequent melting endotherm during the second heating.

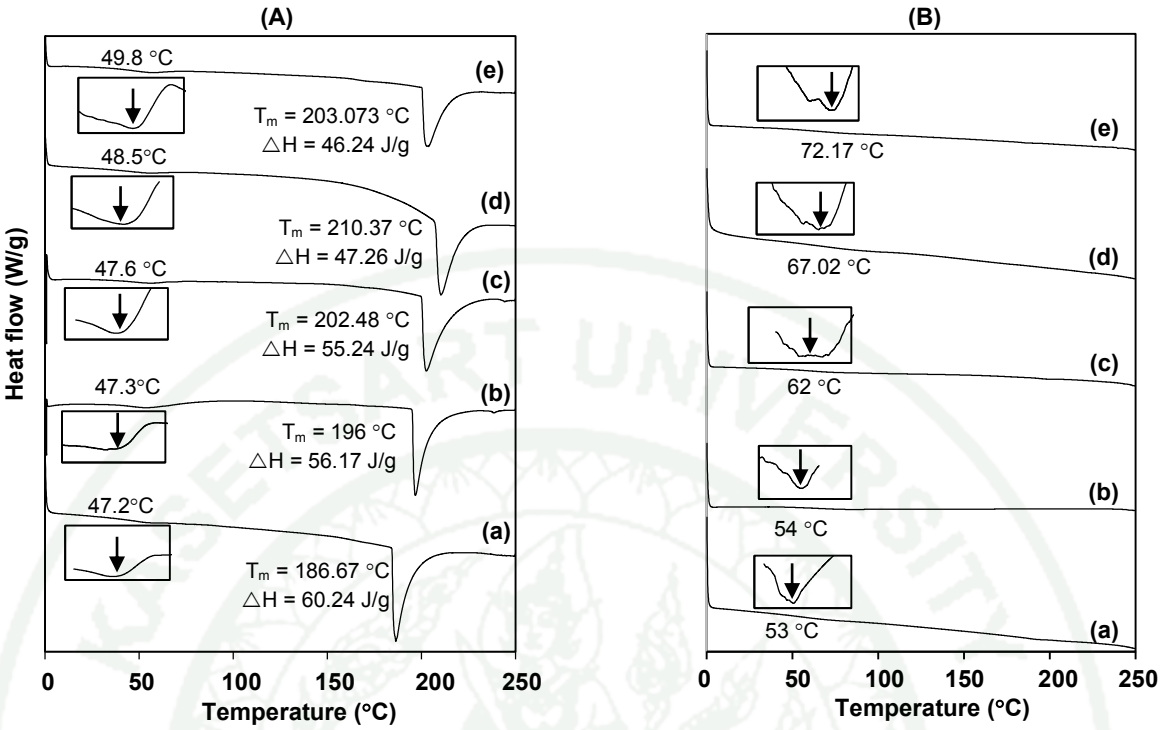

Figure 11 DSC thermograms of (A) first heating scan and (B) second heating scan of different sample films: (a) TPS, (b) TPS/CTS0.5, (c) TPS/CTS1, (d) TPS/CTS1.5 and (e) TPS/CTS2. Insets represent first derivatives of DSC thermograms in the temperature range of (A) 30-65 °C and (B) 30-85 °C

8. Tensile properties of thermoplastic starch/chitosan films

Tensile properties of TPS and TPS/CTS films with various chitosan concentrations were tested after conditioned at 42 ± 2 %RH and 62 ± 2 %RH. At 42 ± 2 %RH, tensile strength (TS) and Young's modulus of TPS film increased by incorporating chitosan with a content of 0.5–2 phs (Fig. 12A and B). In addition, TS and Young's modulus of TPS/CTS films increased with increasing chitosan content, reflecting that the film became stronger and more rigid. On the other hand, elongation at break of TPS film decreased by adding chitosan and the reduction of elongation at break increased with increasing chitosan concentration, implying that extensibility of the film decreased. The augmentation of tensile strength and rigidity as well as the reduction of extensibility of TPS film by adding chitosan could be explained by the

formation of intermolecular hydrogen bonds between starch and chitosan. Pelissari *et al.* (2012) and Xu *et al.* (2005) also reported that tensile strength of cassava starch/chitosan films prepared by two different methods, i.e. blown film extrusion and solution casting, increased with increasing chitosan content, attributing to the formation of intermolecular hydrogen bonding between $–NH_2$ groups present in the structure of chitosan and the –OH groups of cassava starch.

However, TS and Young's modulus of the films stored at 62 ± 2 %RH slightly increased by incorporating chitosan, while elongation at break hardly changed. It might be assumed that the effect of absorbed moisture/water, which could act as a plasticizer was more predominant than that of chitosan. Perdomo *et al.* (2009) also reported that at higher moisture content, water plasticized the cassava starch resulting in decreased glass transition temperature of sample.

TPS and TPS/CTS films conditioned at 62 ± 2 %RH showed lower TS and Young's modulus, but higher elongation at break than those conditioned at 42 ± 2 %RH, reflecting that the films became more flexible when they were stored at higher relative humidity condition. This might be explained by the plasticizing effect of moisture absorbed by the samples. It should be pointed out that the increment of TS and Young's modulus as well as the reduction of elongation at break of the films conditioned at 42 ± 2 %RH were more significantly than the ones conditioned at 62 ± 2 %RH. This result confirmed that the relative humidity of the storage condition or the moisture content of the samples strongly affected the tensile properties of the TPS-based films.

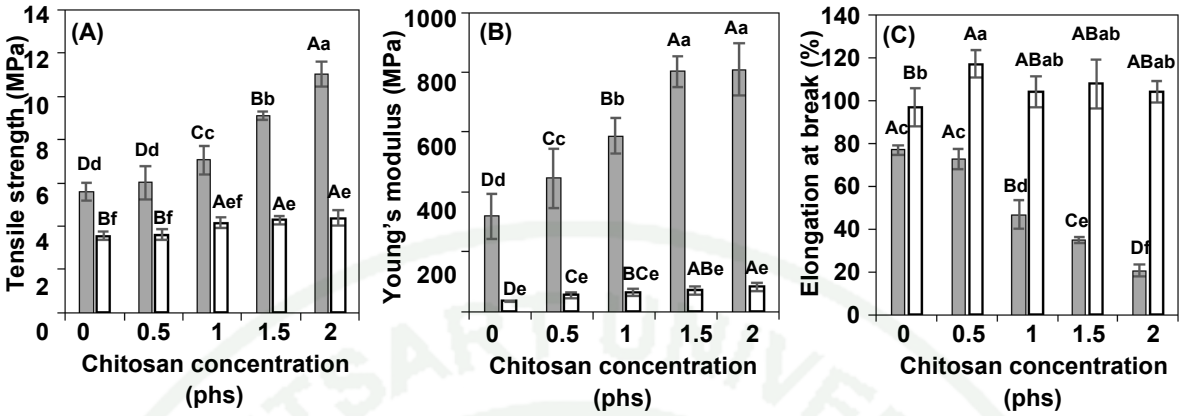

Figure 12 (A) Tensile strength**,** (B) Young's modulus and (C) elongation at break of TPS and TPS/CTS films containing different chitosan concentrations after conditioned at 42 ± 2 %RH (▬) and 62 ± 2 %RH (▭). The data is reported as mean ± SD, $n = 4$. The different capital letters indicate significant difference at $p < 0.05$ (Duncan's new multiple range test) of the data with different chitosan concentration and the different small letters indicate significant difference at $p < 0.05$ (Duncan's new multiple range test) of the data with different sample storage condition.

9. Morphology of thermoplastic starch/chitosan films

Surface morphology of TPS and TPS/CTS films was investigated by SEM technique. TPS film exhibited smooth surface (Fig. 13a), while TPS/CTS films showed rough and porous surfaces (Fig. 13b-e). The addition of chitosan with a content of 0.5 phs hardly affected the surface morphology of TPS film (Fig. 13b); however the film surface morphology was significantly changed when chitosan with higher concentrations, i.e. 1-2 phs was incorporated (Fig 13c-e). The surface roughness of the film containing chitosan with a content in the range of 1-2 phs decreased and the surface matrix became denser with smaller pore size when chitosan content increased. The rough surface of the TPS/CTS films might be a result of the surface coverage of the film with chitosan-rich phase layer since relatively small molecules of chitosan as compared with starch could move to the film surface during

cooling down/solidification. This hypothesis was also confirmed by using ninhydrin assay.

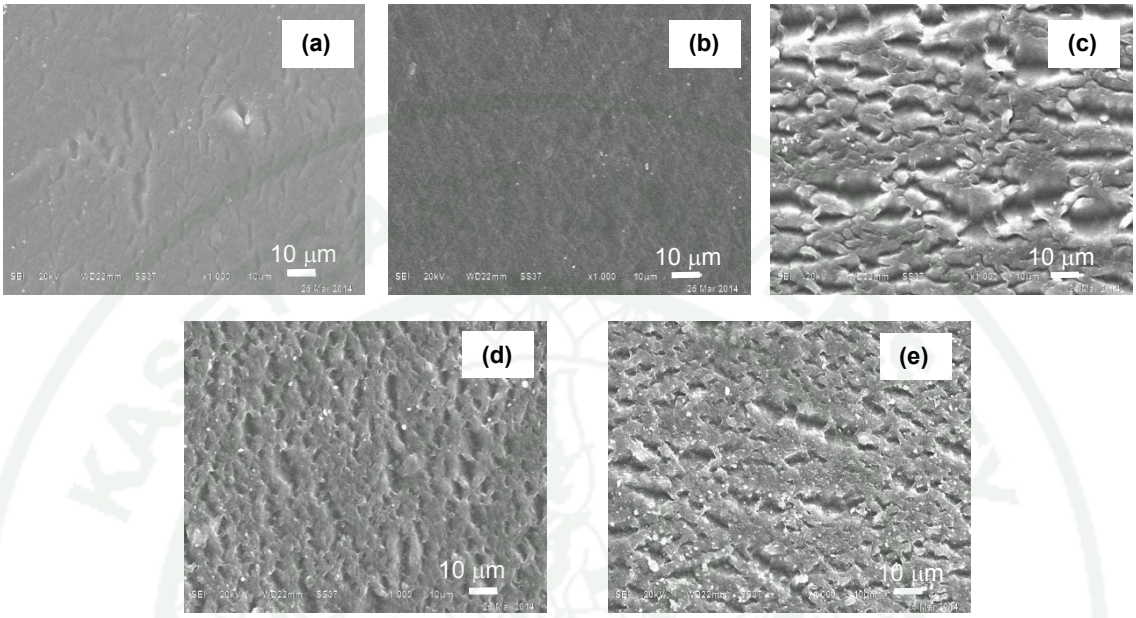

Figure 13 SEM micrographs at film surface of different sample films: (a) TPS, (b) TPS/CTS0.5, (c) TPS/CTS1, (d) TPS/CTS1.5 and (e) TPS/CTS2.

The morphology of sample films at the cross section after testing tensile properties was also observed by SEM. All films showed 2 layers (Fig.14) after passing through the nip roll due to their surface stickiness. The thickness of the monolayer was in the range of 53-120 µm. TPS films showed thicker layer than TPS/CTS films. This result corresponded to the thickness measured by a thickness gage. It suggested that adding chitosan could enhance the blown film extrusion processability so that thinner films were achieved. The addition of chitosan did not show significant changes in the morphology at cross section of the TPS film (Fig. 14). It was probably due to the good interfacial adhesion between starch and chitosan as also reported by Bonilla *et al.* (2013b), who found that the inner structure of wheat starch-chitosan films was uniform suggesting a homogeneous blend.

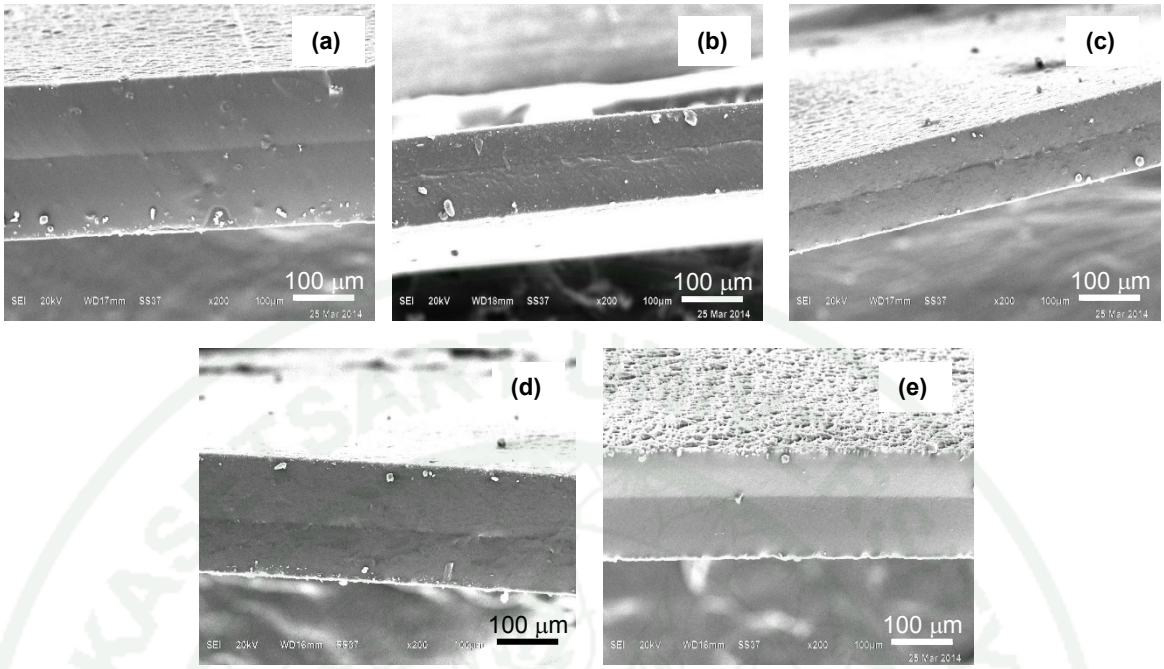

Figure 14 SEM micrographs at cross section area after tensile testing of different sample films: (a) TPS, (b) TPS/CTS0.5, (c) TPS/CTS1, (d) TPS/CTS1.5 and (e) TPS/CTS2.

10. Investigation of the presence of chitosan on the film surface by reaction with ninhydrin

Ninhydrin assay was applied to confirm whether chitosan was presented on the TPS/CTS film surfaces. In general, amino groups of chitosan can form complex with ninhydrin via Schiff base to give blue color (Scheme 1). The formation and stability of the chromophore is dependent on various factors such as temperature and pH of the reaction mixture, duration of heating and reagent concentration. Therefore, the investigation of the presence of chitosan on the film surface by reaction with ninhydrin was performed in the buffer solution with a pH of 5.5 at 100 ° C for 30 sec.

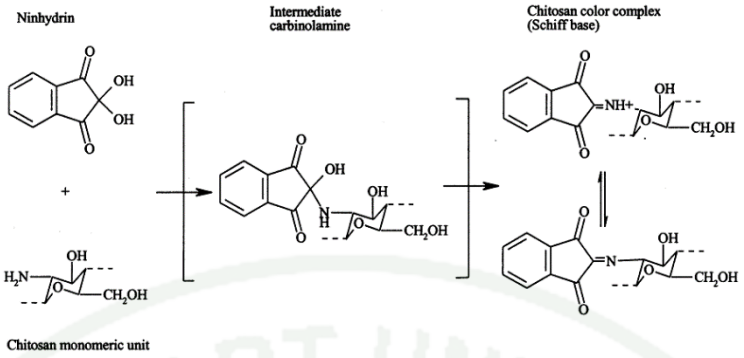

Scheme 1 Proposed reaction of ninhydrin with glucosamine moiety of chitosan to form colored complex.

Source: Sabnis and Block (2000)

Fig. 15 shows that TPS film surface is white, whereas the surface of TPS/CTS films exhibited blue color. The film became darker blue when chitosan concentration increased due to the increasing of amino group content. The result confirmed that chitosan existed on the film surface, which is in agreement with the result from SEM.

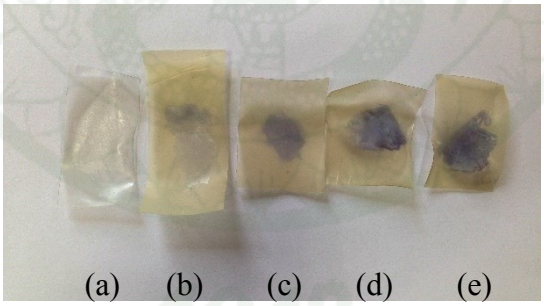

Figure 15 Color change after reaction with ninhydrin of different sample films: (a) TPS, (b) TPS/CTS0.5, (c) TPS/CTS1, (d) TPS/CTS1.5 and (e) TPS/CTS2.

11. Water vapor permeability of thermoplastic starch/chitosan films

Water vapor permeability (WVP) of sample films was determined by a cup method at 52 ± 2 %RH. WVP of TPS film was 36.8 g.mm/m^2.day.atm, while those of TPS/CTS films were in the range of 24.1–30.5 g.mm/m^2.day.atm (Fig. 16). WVP of

TPS/CTS films decreased with increasing chitosan content. The result implied that addition of chitosan could improve water vapor barrier properties of the TPS film or in other words, chitosan could prevent the diffusion of water molecules to pass through the film. This might be explained by the intermolecular hydrogen bond formation between starch and chitosan molecules leading to the dense film matrix. Pelissari *et al.* (2012) also revealed that water vapor permeability of thermoplastic starch/chitosan blown film decreased with increasing chitosan content because of the increased number of interaction between starch molecules and chitosan. Another reason might be related to the formation of thin chitosan layer on the outer film surface, which imparted more hydrophobicity to the films due to the presence of hydrophobic acetyl group (Bangyekan *et al.*, 2006; Vásconez *et al.*, 2009).

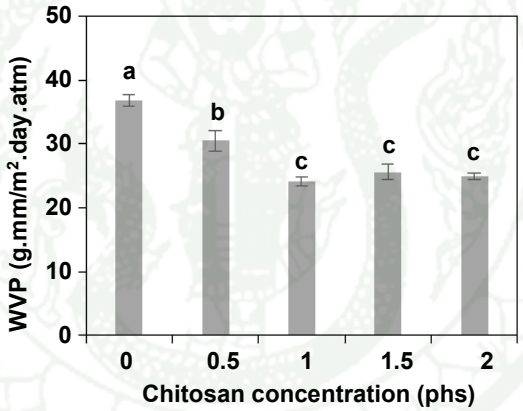

Figure 16 (A) Water vapor permeability of TPS and TPS/CTS films containing different chitosan concentrations. The data is reported as mean ± SD, $n = 3$. The different small letters indicate significant difference at $p < 0.05$ (Duncan's new multiple range test).

12. Water contact angle of thermoplastic starch/chitosan films

Wettability and hydrophobic characteristics of the materials can be evaluated from the water contact angle. A lower water contact angle is generally observed for less hydrophobic materials or the materials with good water wettability. Water contact angle of the sample films was measured at various times for 1 minute. Water

contact angle tended to decrease with increasing time (Fig. 17). TPS film showed water contact angle measured immediately after dropping of 50°, while TPS/CTS films gave higher water contact angles, i.e. in the range of 52 °–78°. This implied that incorporation of chitosan decreased water wettability of the TPS film or improved its hydrophobicity. This result is corresponding to that of Bangyekan *et al.* (2006); they reported that the hydrophobicity of chitosan due to the presence of hydrophobic acetyl groups played an important role in hindering the transportation of water vapor of chitosan-coated cassava starch films. In addition, water contact angle of TPS/CTS films increased with increasing chitosan concentration (Fig. 17). The increase in water contact angle of the films containing chitosan might be a result of the reduction of free hydroxyl group contents due to the hydrogen bond formation between starch and chitosan. Vásconez *et al.* (2009) also reported that hydrogen bond interactions between tapioca starch and chitosan in the chitosan/tapioca starch based edible film and coating reduced the availability of the hydrophilic groups and diminished their interaction with water molecules. This water contact angle information supported the WVP results; water was more difficult to access the surfaces of TPS/CTS films compared with that of TPS film.

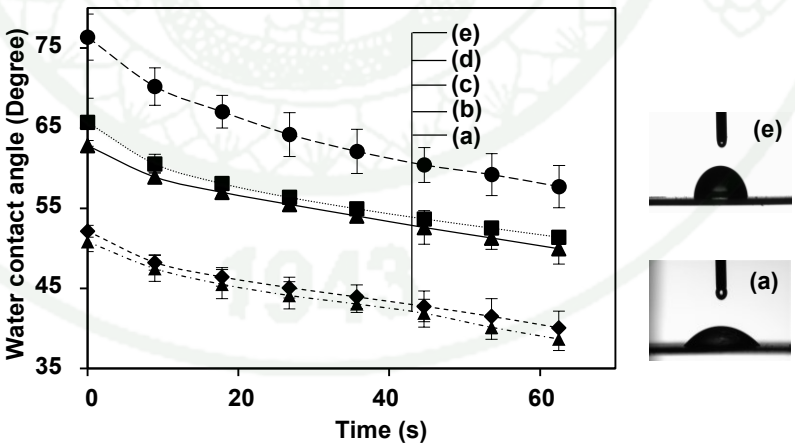

Figure 17 Water contact angle of different sample films: (a) TPS, (b) TPS/CTS0.5, (c) TPS/CTS1, (d) TPS/CTS1.5 and (e) TPS/CTS2. The data is reported as mean ± SD, $n = 3$. The different small letters indicate significant difference at $p < 0.05$ (Duncan's new multiple range test).

13. Oxygen permeability of thermoplastic starch/chitosan films

Oxygen permeability (OP) of TPS and TPS/CTS films was measured at ambient temperature and 0 %RH. OP of TPS film was 137.3 CC.mm/m^2.day.bar, while those of TPS/CTS films were in the range of 82.3-29.13 CC.mm/m^2.day.bar (Fig. 18). The result implied that oxygen barrier property of TPS film was improved by adding chitosan. This might be explained by the intermolecular hydrogen bond formation between starch and chitosan chains leading to reduced chain mobility and decreased free volume of polymer matrix. Shen *et al.* (2010) has confirmed that chitosan could form inter-molecular hydrogen bonds with starch in the sweet potato/chitosan cast film, which limited the inter-molecular chain mobility and decreased free volume between starch molecules, contributing to the decrease of OP. In addition, the relatively high crystallinity of chitosan network on the film surface is another reason for OP reduction. Mazeau *et al.* (1994) reported that the chitosan molecules are stabilized by intra-molecular hydrogen bonds and its crystalline structure is held together by a network of intermolecular hydrogen bonds.

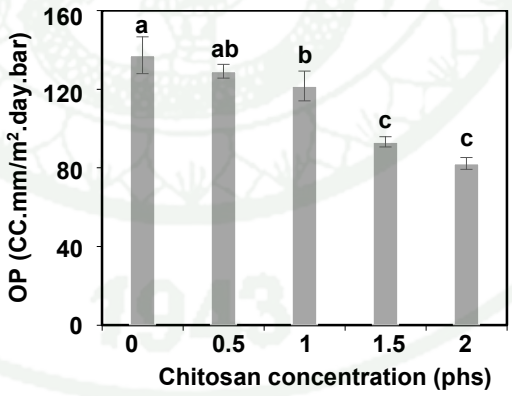

Figure 18 Oxygen permeability of TPS and TPS/CTS films containing different chitosan concentrations. The data is reported as mean ± SD, $n = 3$. The different small letters indicate significant difference at $p < 0.05$ (Duncan's new multiple range test).

CONCLUSIONS AND RECOMMENDATIONS

Conclusions

TPS/CTS compounds were prepared using a twin-screw extruder and then converted into a film by blown film extrusion. FTIR and XRD results showed that starch could form hydrogen bond interaction with chitosan resulting in decreased V-type crystallinity and positive effect to tensile and barrier properties of the film. The addition of 0.5-2 phs of chitosan improved strength (tensile strength increased ≈ 8-97%), stiffness (Young's modulus increased ≈ 40-154%), water vapor barrier property (WVP decreased ≈ 17-35%), oxygen barrier property (OP decreased ≈ 6-40%) and thermal stability as well as reduced water absorption and surface stickiness of the TPS film. However, extensibility of TPS film decreased (elongation at break decreased ≈ 5-73%) by incorporating chitosan. SEM observations confirmed the homogeneity of the film matrix and the film surface coverage with a thin layer of chitosan. Glass transition temperature of starch in the film increased by incorporating chitosan. The film became yellow and opaque as well as showed greater UV absorption when chitosan was loaded.

Recommendations

1. Moisture sensitivity and surface stickiness of TPS/CTS films should be reduced because they caused film shrinkage, two-layered film and difficulty in properties testing. The possible and easy methods have been recommended here, i.e. blending TPS/CTS compounds with more hydrophobic polymers or decreasing their plasticizer content.

2. Antimicrobial activity of TPS/CTS films should be tested in the future to widen the application ranges of this TPS/CTS film, particularly in food packaging since antimicrobial activity is one of the outstanding characteristics of chitosan.

LITERATURE CITED

Anchisi, C., M. C. Meloni and A. M. Maccioni. 2006. Chitosan Beads Loaded with Essential Oils in Cosmetic Formulations. **Journal of Cosmetic Science.** 57 (3): 205-214.

Avérous, L. 2004. Biodegradable Multiphase Systems Based on Plasticized Starch: A Review. **Journal of Macromolecular Science, Part C.** 44 (3): 231-274.

Avérousa, L., C. Fringantb and L. Moro. 2001. Starch-Based Biodegradable Materials Suitable for Thermoforming Packaging. **Starch/Stärke.** 53: 368–371.

Bangyekan, C., D. Aht-Ong and K. Srikulkit. 2006. Preparation and Properties Evaluation of Chitosan-Coated Cassava Starch Films. **Carbohydrate Polymers.** 63 (1): 61-71.

Bertolini, A. C. 2010. Trends in Starch Applications. A. C. Bertolini, eds. **Starches: Characterization, Properties, and Applications.** CRC Press.

Blanshard, J. M. V. 1987. Starch Granule Structure and Function: A Physicochemical Approach. 14-54. T. Galliard, eds. **Starch: Properties and Potential.** John Wiley & Sons, New York.

Bonilla, J., L. Atarés, M. Vargas and A. Chiralt. 2013a. Properties of Wheat Starch Film-Forming Dispersions and Films as Affected by Chitosan Addition. **Journal of Food Engineering.** 114 (3): 303-312.

Bonilla, J., E. Talón, L. Atarés, M. Vargas and A. Chiralt. 2013b. Effect of the Incorporation of Antioxidants on Physicochemical and Antioxidant Properties of Wheat Starch–Chitosan Films. **Journal of Food Engineering.** 118 (3): 271-278.

Bonilla, J., E. Fortunati, M. Vargas, A. Chiralt and J. M. Kenny. 2013c. Effects of Chitosan on the Physicochemical and Antimicrobial Properties of Pla Films. **Journal of Food Engineering.** 119 (2): 236-243.

Bourtoom, T. and M. S. Chinnan. 2008. Preparation and Properties of Rice Starch–Chitosan Blend Biodegradable Film. **LWT - Food Science and Technology.** 41 (9): 1633-1641.

Brandelero, R. P., M. V. Grossmann and F. Yamashita. 2012. Films of Starch and Poly(Butylene Adipate Co-Terephthalate) Added of Soybean Oil (So) and Tween 80. **Carbohydrate Polymers.** 90 (4): 1452-1460.

Brück, W. M., J. W. Slater and B. F. Carney. 2010. Chitin and Chitosan from Marine Organisms. 666. S. Kim, eds. **Chitin, Chitosan, Oligosaccharides and Their Derivatives: Biological Activities and Applications.** CRC Press.

Carvalho, A. J. F. 2008. Starch-Major Sources, Properties and Applications as Thermoplastic Materials. M. N. Belgacem and A. Gandini, eds. **Monomers, Polymers and Composites from Renewable Resources.** Elsevier Science, Amsterdam.

Chang, P. R., R. Jian, J. Yu and X. Ma. 2010. Fabrication and Characterisation of Chitosan Nanoparticles/Plasticised-Starch Composites. **Food Chemistry.** 120 (3): 736-740.

Chen, J. L. and Y. Zhao. 2012. Effect of Molecular Weight, Acid, and Plasticizer on the Physicochemical and Antibacterial Properties of Beta-Chitosan Based Films. **Journal of Food Science.** 77 (5): E127-136.

Chen, P., L. Zhang and F. Cao. 2005. Effects of Moisture on Glass Transition and Microstructure of Glycerol-Plasticized Soy Protein. **Macromolecular Bioscience.** 5 (9): 872-880.

Chillo, S., S. Flores, M. Mastromatteo, A. Conte, L. Gerschenson and M. A. Del Nobile. 2008. Influence of Glycerol and Chitosan on Tapioca Starch-Based Edible Film Properties. **Journal of Food Engineering.** 88 (2): 159-168.

Cissé, M., D. Montet, G. Loiseau and M.-N. Ducamp-Collin. 2012. Influence of the Concentrations of Chitosan and Glycerol on Edible Film Properties Phowed by Response Rurface Methodology. **Journal of Polymers and the Environment.** 20 (3): 830-837.

Colonna, P., A. Buleon and C. Mercier. 1987. Physically Modified Starches. 79 - 115. T. Galliard, eds. **Starch: Properties and Potential.** John Wily & Sons, Chichester.

Cyras, V. P., L. B. Manfredi, M.-T. Ton-That and A. Vázquez. 2008. Physical and Mechanical Properties of Thermoplastic Starch/Montmorillonite Nanocomposite Films. **Carbohydrate Polymers.** 73 (1): 55-63.

Dean, K., L. Yu and D. Y. Wu. 2007. Preparation and Characterization of Melt-Extruded Thermoplastic Starch/Clay Nanocomposites. **Composites Science and Technology.** 67 (3-4): 413-421.

Dean, K., P. Sangwan, C. Way, X. Zhang, V. P. Martino, F. Xie, P. J. Halley, E. Pollet and L. Avérous. 2013. Glycerol Plasticised Chitosan: A Study of Biodegradation Via Carbon Dioxide Evolution and Nuclear Magnetic Resonance. **Polymer Degradation and Stability.** 98 (6): 1236-1246.

Delval, F., G. Crini, S. Bertini, N. Morin-Crini, P.-M. Badot, J. Vebrel and G. Torri. 2004. Characterization of Crosslinked Starch Materials with Spectroscopic Techniques. **Journal of Applied Polymer Science.** 93 (6): 2650-2663.

Dodane, V. and V. D. Vilivalam. 1998. Pharmaceutical Applications of Chitosan. **Pharmaceutical Science & Technology Today.** 1 (6): 246-253.

Dutta, P. K., S. Tripathi, G. K. Mehrotra and J. Dutta. 2009. Perspectives for Chitosan Based Antimicrobial Films in Food Applications. **Food Chemistry.** 114 (4): 1173-1182.

Eichhorn, K.-J., A. Fahmi, G. Adam and M. Stamm. 2003. Temperature-Dependent Ftir Spectroscopic Studies of Hydrogen Bonding of the Copolymer Poly(Styrene-B-4-Vinylpyridine) with Pentadecylphenol. **Journal of Molecular Structure.** 661-662 161-170.

El-Sawy, N. M., H. A. Abd El-Rehim, A. M. Elbarbary and E.-S. A. Hegazy. 2010. Radiation-Induced Degradation of Chitosan for Possible Use as a Growth Promoter in Agricultural Purposes. **Carbohydrate Polymers.** 79 (3): 555-562.

French, D. 1973. Chemical and Physical Properties of Starch. **Journal of Animal Science.** 37: 1048-1061.

Gallant, D. J., B. Bouchet and P. M. Baldwin. 1997. Microscopy of Starch: Evidence of a New Level of Granule Organization. **Carbohydrate Polymers.** 32: 177-191.

Giovino, C., I. Ayensu, J. Tetteh and J. S. Boateng. 2012. Development and Characterisation of Chitosan Films Impregnated with Insulin Loaded Peg-B-Pla Nanoparticles (Nps): A Potential Approach for Buccal Delivery of Macromolecules. **Int J Pharm.** 428 (1-2): 143-151.

Hulleman, S. H. D., W. Helbert and H. Chanzy. 1996. Single Crystals of V Amylose Complexed with Glycerol. **International Journal of Biological Macromolecules.** 18 (1–2): 115-122.

Huneault, M. A. and H. Li. 2012. Preparation and Properties of Extruded Thermoplastic Starch/Polymer Blends. **Journal of Applied Polymer Science.** 126 (S1): E96-E108.

Imberty, A. and S. Perez. 1988. A Revisit to the Three-Dimensional Structure of B-Type Starch. **Biopolymers.** 27 (8): 1205-1221.

Kaewtatip, K. and J. Thongmee. 2013. The Effects of Cross-Linked Starch on the Properties of Thermoplastic Starch. **Materials & Design.** 45: 586-589.

Kean, T. and M. Thanou. 2010. Biodegradation, Biodistribution and Toxicity of Chitosan. **Advanced Drug Delivery Reviews.** 62 (1): 3-11.

Kössler, I., F. U. Chemie and C. A. Věd. 1990. Infrared-Absorption Spectroscopy. 371-402. J. I. K., eds. **Polymers: Polymer Characterization and Analysis.** Wiley

Li, Q., E. T. Dunn, E. W. Grandmaison and M. F. A. Goosen. 1996. Applications and Properties of Chitosan. 336. M. F. A. Goosen, eds. **Applications of Chitan and Chitosan.** CRC Press.

Martínez-Camacho, A. P., M. O. Cortez-Rocha, J. M. Ezquerra-Brauer, A. Z. Graciano-Verdugo, F. Rodriguez-Félix, M. M. Castillo-Ortega, M. S. Yépiz-Gómez and M. Plascencia-Jatomea. 2010. Chitosan Composite Films: Thermal, Structural, Mechanical and Antifungal Properties. **Carbohydrate Polymers.** 82 (2): 305-315.

Mazeau, K., W. T. Winter and H. Chanzy. 1994. Molecular and Crystal Structure of a High-Temperature Polymorph of Chitosan from Electron Diffraction Data. **Macromolecules.** 27 (26): 7606-7612.

Mościcki, L., M. Mitrus, A. Wójtowicz, T. Oniszczuk, A. Rejak and L. Janssen. 2012. Application of Extrusion-Cooking for Processing of Thermoplastic Starch (Tps). **Food Research International.** 47 (2): 291-299.

Pelissari, F. M., F. Yamashita and M. V. E. Grossmann. 2011. Extrusion Parameters Related to Starch/Chitosan Active Films Properties. **International Journal of Food Science & Technology.** 46 (4): 702-710.

Pelissari, F. M., M. V. Grossmann, F. Yamashita and E. A. Pineda. 2009. Antimicrobial, Mechanical, and Barrier Properties of Cassava Starch-Chitosan Films Incorporated with Oregano Essential Oil. **Journal of Agricultural and Food Chemitry.** 57 (16): 7499-7504.

Pelissari, F. M., F. Yamashita, M. A. Garcia, M. N. Martino, N. E. Zaritzky and M. V. E. Grossmann. 2012. Constrained Mixture Design Applied to the Development of Cassava Starch–Chitosan Blown Films. **Journal of Food Engineering.** 108 (2): 262-267.

Perdomo, J., A. Cova, A. J. Sandoval, L. García, E. Laredo and A. J. Müller. 2009. Glass Transition Temperatures and Water Sorption Isotherms of Cassava Starch. **Carbohydrate Polymers.** 76 (2): 305-313.

Pillai, C. K. S., W. Paul and C. P. Sharma. 2009. Chitin and Chitosan Polymers: Chemistry, Solubility and Fiber Formation. **Progress in Polymer Science.** 34 (7): 641-678.

Prachayawarakorn, J., P. Sangnitidej and P. Boonpasith. 2010. Properties of Thermoplastic Rice Starch Composites Reinforced by Cotton Fiber or Low-Density Polyethylene. **Carbohydrate Polymers.** 81 (2): 425-433.

Richardson, S. W., H. J. Kolbe and R. Duncan. 1999. Potential of Low Molecular Mass Chitosan as a DNA Delivery System: Biocompatibility, Body

Distribution and Ability to Complex and Protect DNA. **International Journal of Pharmaceutics.** 178 (2): 231-243.

Rindlav-Westling, A. s., M. Stading, A.-M. Hermansson and P. Gatenholm. 1998. Structure, Mechanical and Barrier Properties of Amylose and Amylopectin Films. **Carbohydrate Polymers.** 36 (2–3): 217-224.

Rodríguez-Núñez, J. R., J. López-Cervantes, D. I. Sánchez-Machado, B. Ramírez-Wong, P. Torres-Chavez and M. O. Cortez-Rocha. 2012. Antimicrobial Activity of Chitosan-Based Films against Salmonella Typhimurium and Staphylococcus Aureus. **MouraInternational Journal of Food Science & Technology.** 47 (10): 2127-2133.

Röper, H. and B. Elvers. 2008. **Ullman's Encyclopedia of Industrial Chemistry** John Wiley & Sons, New York.

Roz, A., A. Carvalho, A. Gandini and A. Curvelo. 2006. The Effect of Plasticizers on Thermoplastic Starch Compositions Obtained by Melt Processing. **Carbohydrate Polymers.** 63 (3): 417-424.

Sabnis, S. and L. H. Block. 2000. Chitosan as an Enabling Excipient for Drug Delivery Systems: I. Molecular Modifications. **International Journal of Biological Macromolecules.** 27 (3): 181-186.

Sakurai, K., T. Maegawa and T. Takahashi. 2000. Glass Transition Temperature of Chitosan and Miscibility of Chitosan/Poly(N-Vinyl Pyrrolidone) Blends. **Polymer.** 41 (19): 7051-7056.

Shen, X. L., J. M. Wu, Y. Chen and G. Zhao. 2010. Antimicrobial and Physical Properties of Sweet Potato Starch Films Incorporated with Potassium Sorbate or Chitosan. **Food Hydrocolloids.** 24 (4): 285-290.

Shi, R., Q. Liu, T. Ding, Y. Han, L. Zhang, D. Chen and W. Tian. 2007. Ageing of Soft Thermoplastic Starch with High Glycerol Content. **Journal of Applied Polymer Science.** 103 (1): 574-586.

Shirai, M. A., M. V. Grossmann, S. Mali, F. Yamashita, P. S. Garcia and C. M. Muller. 2013a. Development of Biodegradable Flexible Films of Starch and Poly(Lactic Acid) Plasticized with Adipate or Citrate Esters. **Carbohydrate Polymers.** 92 (1): 19-22.

Shirai, M. A., J. B. Olivato, P. S. Garcia, C. M. Muller, M. V. Grossmann and F. Yamashita. 2013b. Thermoplastic Starch/Polyester Films: Effects of Extrusion Process and Poly (Lactic Acid) Addition. **Materials Science and Engineering C.** 33 (7): 4112-4117.

Shujun, W., Y. Jiugao and Y. Jinglin. 2006. Preparation and Characterization of Compatible and Degradable Thermoplastic Starch/Polyethylene Film. **Journal of Polymers and the Environment.** 14 (1): 65-70.

Skrovanek, D. J., S. E. Howe, P. C. Painter and M. M. Coleman. 1985. Hydrogen Bonding in Polymers: Infrared Temperature Studies of an Amorphous Polyamide. **Macromolecules.** 18 (9): 1676-1683.

Soest, J. J. G. and P. Essers. 1997. Influence of Amylose-Amylopectin Ratio on Properties of Extruded Starch Plastic Sheets. **Journal of Macromolecular Science, Part A.** 34 (9): 1665-1689.

Stagner, J., V. Dias Alves, R. Narayan and A. Beleia. 2011. Thermoplasticization of High Amylose Starch by Chemical Modification Using Reactive Extrusion. **Journal of Polymers and the Environment.** 19 (3): 589-597.

Teixeira, E. M., A. A. S. Curvelo, A. C. Corrêa, J. M. Marconcini, G. M. Glenn and L. H. C. Mattoso. 2012. Properties of Thermoplastic Starch from Cassava

Bagasse and Cassava Starch and Their Blends with Poly (Lactic Acid). **Industrial Crops and Products.** 37 (1): 61-68.

Thunwall, M., V. Kuthanova, A. Boldizar and M. Rigdahl. 2008. Film Blowing of Thermoplastic Starch. **Carbohydrate Polymers.** 71 (4): 583-590.

Vargas, M., A. Albors, A. Chiralt and C. González-Martínez. 2006. Quality of Cold-Stored Strawberries as Affected by Chitosan–Oleic Acid Edible Coatings. **Postharvest Biology and Technology.** 41 (2): 164-171.

Vásconez, M. B., S. K. Flores, C. A. Campos, J. Alvarado and L. N. Gerschenson. 2009. Antimicrobial Activity and Physical Properties of Chitosan–Tapioca Starch Based Edible Films and Coatings. **Food Research International.** 42 (7): 762-769.

Xu, Y. X., K. M. Kim, M. A. Hanna and D. Nag. 2005. Chitosan–Starch Composite Film: Preparation and Characterization. **Industrial Crops and Products.** 21 (2): 185-192.

Zasypkin, D. V., V. P. Yuryev, V. V. Alexeyev and V. B. Tolstoguzov. 1992. Mechanical Properties of the Products Obtained by the Thermoplastic Extrusion of Potato Starch-Soybean Protein Mixtures. **Carbohydrate Polymers.** 18 (2): 119-124.

Zeng, D., J. Wu and J. F. Kennedy. 2008. Application of a Chitosan Flocculant to Water Treatment. **Carbohydrate Polymers.** 71 (1): 135-139.

Zhong, Y., X. Song and Y. Li. 2011. Antimicrobial, Physical and Mechanical Properties of Kudzu Starch–Chitosan Composite Films as a Function of Acid Solvent Types. **Carbohydrate Polymers.** 84 (1): 335-342.

Zullo, R. and S. Iannace. 2009. The Effects of Different Starch Sources and Plasticizers on Film Blowing of Thermoplastic Starch: Correlation among

Process, Elongational Properties and Macromolecular Structure. **Carbohydrate Polymers.** 77 (2): 376-383.

APPENDIX

Appendix Table 1 Color measurement of TPS/CTS films.

Sample	Hunter color value		
	L^*	a^*	b^*
TPS	93.98±0.23[a]	-0.06±0.01[d]	1.22±0.05[e]
TPS/CTS0.5	93.22±0.44[b]	0.02±0.01[c]	3.34±0.08[d]
TPS/CTS1	92.80±0.2[b]	0.04±0.01[c]	3.58±0.06[c]
TPS/CTS1.5	91.76±0.10[c]	0.08±0.01[b]	3.72±0.07[b]
TPS/CTS2	89.98±0.16[d]	0.18±0.01[a]	4.32±0.07[a]

The data is reported as mean ± SD, $n = 3$. The different small letters indicate significant difference at $p < 0.05$ (Duncan's new multiple range test).

Appendix Table 2 Tensile properties of TPS/CTS films.

Sample	Tensile strength (MPa)	Young's modulus (MPa)	Elongation at break (%)
42% RH			
Pure TPS	5.6±0.4^{d}	318.2±76.1^{d}	76.9±2.1^{c}
TPS/CTS0.5	6.0±0.8^{d}	445.3±100.6^{c}	72.7±4.8^{c}
TPS/CTS1	7.1±0.7^{c}	587.1±59.6^{b}	46.7±6.9^{d}
TPS/CTS1.5	9.1±0.2^{b}	803.1±51.2^{a}	34.5±1.4^{e}
TPS/CTS2	11.0±0.6^{a}	808.5±87.3^{a}	20.6±2.9^{f}
62 %RH			
TPS	3.6±0.0^{f}	36.5±1.8^{e}	99.5±7.8^{b}
TPS/CTS0.5	3.7±0.2^{f}	53.4±10.4^{e}	111.0±2.6^{a}
TPS/CTS1	4.1±0.2^{ef}	67.0±8.7^{e}	104.0±8.3^{ab}
TPS/CTS1.5	4.4±0.1^{e}	76.2±10.8^{e}	107.4±13.1^{ab}
TPS/CTS2	4.5±0.4^{e}	79.2±12.5^{e}	102.3±3.2^{ab}

The data is reported as mean ± SD, $n = 4$. The different small letters indicate significant difference at $p < 0.05$ (Duncan's new multiple range test).

Appendix Table 3 Water vapor permeability of TPS/CTS films.

Sample	Water vapor permeability ($g.mm/m^2.day.atm$)
TPS	36.81 ± 0.91^a
TPS/CTS0.5	34.13 ± 0.74^b
TPS/CTS1	30.53 ± 1.67^c
TPS/CTS1.5	25.64 ± 1.13^c
TPS/CTS2	24.94 ± 0.52^c

The data is reported as mean ± SD, $n = 3$. The different small letters indicate significant difference at $p < 0.05$ (Duncan's new multiple range test).

Appendix Table 4 Oxygen permeability of TPS/CTS films.

Sample	Oxygen permeability ($CC.mm/m^2.day.bar$)
TPS	137.3 ± 9.33^{a}
TPS/CTS0.5	129.13 ± 3.48^{ab}
TPS/CTS1	121.63 ± 7.55^{b}
TPS/CTS1.5	93.18 ± 2.6^{c}
TPS/CTS2	82.30 ± 2.98^{c}

The data is reported as mean ± SD, $n = 3$. The different small letters indicate significant difference at $p < 0.05$ (Duncan's new multiple range test).

Appendix Table 5 Thickness of TPS and TPS/CTS films.

Sample	Thickness (μm)
TPS	216.8±10[a]
TPS/CTS0.5	183.5±10[b]
TPS/CTS1	157.5±12[c]
TPS/CTS1.5	150.7±4[c]
TPS/CTS2	132.9±2[d]

The data is reported as mean ± SD, $n = 4$. The different small letters indicate significant difference at $p < 0.05$ (Duncan's new multiple range test).

Appendix Table 6 Percent of weight loss at 250 °C and T_d of starch in TPS and TPS/CTS films.

Sample	Weight loss (250 °C)	T_d (°C)
TPS	20.7±0.28[a]	299.65±0.28[a]
TPS/CTS0.5	18.45±3.61[ab]	299.55±0.35[a]
TPS/CTS1	17.2±2.12[ab]	299.3±1.84[a]
TPS/CTS1.5	13.2±4[b]	301.4±1.56[a]
TPS/CTS2	12±1.98[b]	300.45±0.21[4]

The data is reported as mean ± SD, *n = 2*. The different small letters indicate significant difference at $p < 0.05$ (Duncan's new multiple range test).

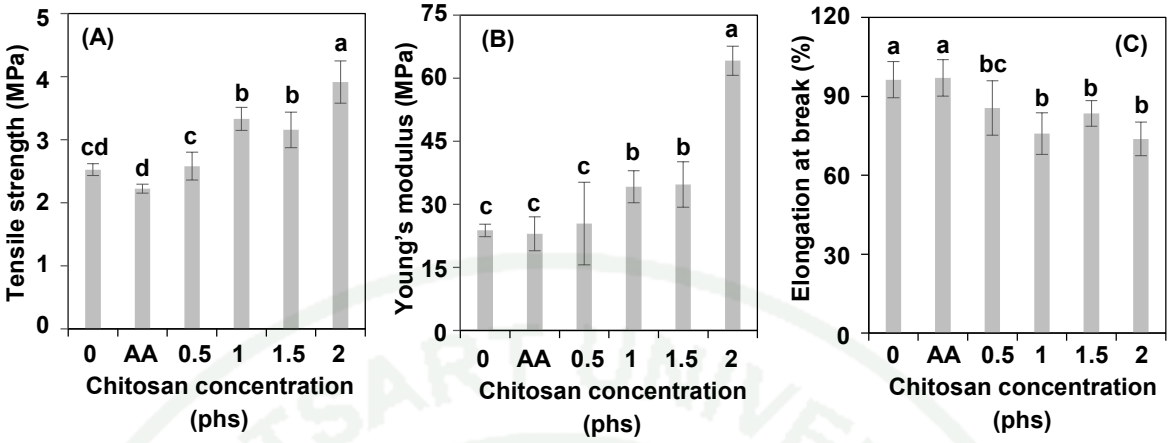

Appendix Figure 1 (A) Tensile strength**,** (B) Young's modulus and (C) elongation at break of TPS, TPS/acid acetic (AA) and TPS/CTS films containing different chitosan concentrations. The data is reported as mean ± SD, $n = 4$. The different small letters indicate significant difference at $p < 0.05$ (Duncan's new multiple range test).

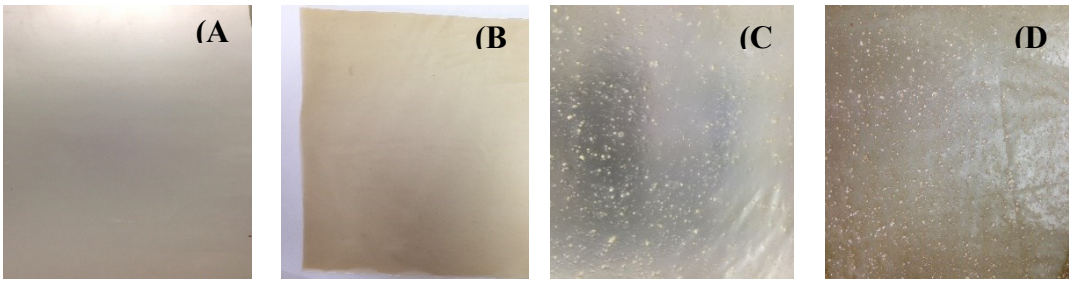

Appendix Figure 2 Photographs of blown films from (A) mixture of cassava starch and glycerol, (B) mixture of cassava starch, glycerol and chitosan solution after drying, (C) mixture of cassava starch and chitosan solution after drying and mixing with glycerol and (D) mixture of cassava starch, glycerol and chitosan flakes.

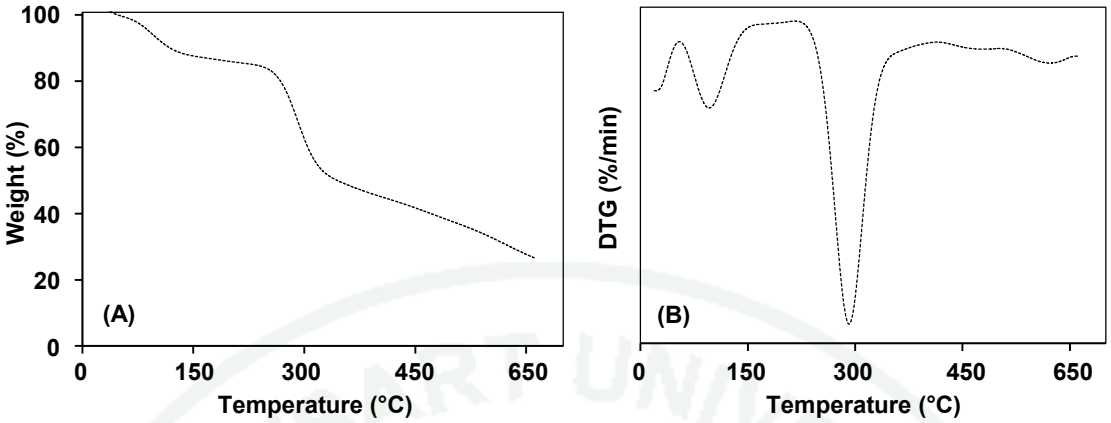

Appendix Figure 3 (A) TGA and (B) DTG thermograms of chitosan flakes.

CURRICULUM VITAE

NAME : Mr. Khanh Minh Dang

BIRTH DATE : August 23, 1989

BIRTH PLACE : Binh Duong, Vietnam

EDUCATION	**YEAR**	**INSTITUE**	**DEGREE**
	2011	Saigon Technology Univ.	B.Eng.

SCHOLARSHIP : Scholarships for International Graduate Student 2012 from Faculty o Agro-Industry, Kasetsart University